Seismic Vulnerability Assessment of Un-reinforced Masonry Buildings Using Capacity Spectrum-based Method

By

Vishwash Rukwal

231370720020

UNDER THE ESTEEMED GUIDANCE OF

Dr. Kaushik Gondaliya

Assistant Professor

School of Engineering and Technology

Co-Guided By

Prof. (Dr.) Jignesh A. Amin

Professor

School of Engineering and Technology

A Thesis Submitted to

Gujarat Technological University in Partial Fulfilment of the Requirement for

The Master of Engineering Degree in Civil (Structural Engineering)

May 2025

Gujarat Technological University

School of Engineering and Technology

Chandkheda, Ahmedabad-382424

CERTIFICATE

This is to certify that research work embodied in the dissertation titled **"Seismic Vulnerability assessment of Un-reinforced Masonry Buildings Using Capacity Spectrum-based Method"** was carried out by **Vishwash Rukwal** bearing **Enrollment No: 231370720020** at GTU - School of Engineering and Technology (Institute Code - 137) for partial fulfillment of **Dissertation Phase 2 - 3740002** in Master of Engineering degree in **Civil Engineering (Structural Engineering)** to be awarded by Gujarat Technological University. This research work has been carried out by him under my supervision and guidance. In my opinion, the submitted work has reached the level required for being accepted for examination.

Date:23th APRIL,2025

Place: Ahmedabad

Signature and Name of Guide   **Signature and Name of Co-Guide**

Dr. Kaushik Gondaliya   **Dr. Jignesh A. Amin**

Assistant Professor,   **Professor**

GTU-SET   **GTU-SET**

Signature and Name of Director

Prof. (Dr.) Jignesh A. Amin

Director, GTU-SET

COMPLIANCE CERTIFICATE

This is to certify that the research work embodied in this dissertation titled **"Seismic Vulnerability assessment of Un-reinforced Masonry Buildings Using Capacity Spectrum-based Method"** was carried out by **Vishwash Rukwal Enrollment No: 231370720020** at GTU - School of Engineering and Technology (Institute Code - 137) for partial fulfillment of Master of Engineering degree in **Civil Engineering (Structural Engineering)** to be awarded by Gujarat Technological University. He has complied to the comments given by the Dissertation Phase-I as well as Mid Semester Thesis Reviewer to my satisfaction.

Date: 23th APRIL, 2025
Place: Ahmedabad

Signature and Name of Student   **Signature and Name of Guide**

Vishwash Rukwal   **Dr. Kaushik Gondaliya**

231370720020   **Assistant Professor, GTU-SET**

Signature and Name of Co-Guide

Dr. Jignesh A. Amin

Professor, GTU-SET

THESIS APPROVAL CERTIFICATE

This is to certify that research work embodied in this thesis entitled "**Seismic Vulnerability Assessment of Un-reinforced Masonry Buildings Using Capacity Spectrum-based Method**" was carried out by (**VISHWASH RUKWAL 231370720020**) at (**SCHOOL OF ENGINEERING AND TECHNOLOGY-137**) is approved for the degree of Master of Engineering in **Civil engineering (Structural Engineering)** by Gujarat Technological University.

Date:

Place:

Examiner's Sign and Name:

(-------------------------------)   (-------------------------------)

UNDERTAKING ABOUT ORIGINALITY OF WORK

We hereby certify that we are the sole authors of this thesis and that neither any part of this thesis nor the whole of the thesis has been submitted for a degree to any other University or Institution. We certify that, to the best of our knowledge, the current thesis does not infringe upon anyone's copyright nor violate any proprietary rights and that any ideas, techniques, quotations or any other material from the work of other people included in our thesis, published or otherwise, are fully acknowledged in accordance with the standard referencing practices. Furthermore, to the extent that we have included copyrighted material that surpasses the boundary of fair dealing within the meaning of the Indian Copyright (Amendment) Act 2012, we certify that we have obtained a written permission from the copyright owner(s) to include such material(s) in the current thesis and have included copies of such copyright clearances to our appendix. We declare that this is a true copy of thesis, including any final revisions, as approved by thesis review committee. We have checked write up of the present thesis using anti-plagiarism database and it is in allowable limit. Even though later on in case of any complaint pertaining of plagiarism, we are sole responsible for the same and we understand that as per UGC norms, University can even revoke Master of Engineering degree conferred to the student submitting this thesis.

Date: - 23th April 2025

Signature and Name of Student   **Signature of Name of Guide**

Vishwash Rukwal   **Dr. Kaushik Gondaliya**

Enrollment No: 231370720020   **Institute Code:137**

Signature and Name of Co-Guide

Dr. Jignesh A. Amin

Professor, GTU-SET

ACKNOWLEDGEMENT

ABSTRACT

Masonry structures, composed of individual units such as bricks, stones, or concrete blocks bound by mortar, are integral to global construction due to their strength, durability, and aesthetic appeal. In India, particularly in Jammu and Kashmir, which falls in seismic zone IV and V their traditional masonry buildings showcase a rich architectural heritage, often incorporating local materials and techniques that respond to the region's climatic conditions. This study focuses on assessing the seismic vulnerability of unreinforced masonry (URM) buildings, which are particularly susceptible to earthquake-induced damage. Utilizing the Finite element method approach, we will design and analyze the URM Building in the Dlubal Rfem-6 advanced structural engineering software, which allows us to Design and perform pushover analysis. Also, we conduct a thorough evaluation of a selected two Story URM building using Capacity Spectrum Method, allowing for a detailed understanding of the building's response to seismic forces using Indian Standards. Additionally, the study identifies the predominant failure modes associated with the structural configurations analyzed, providing valuable information for improving design practices and enhancing resilience against seismic events. The findings will not only contribute to the safety and structural integrity of existing structures in seismically active regions but also inform future architectural practices that honor traditional construction while improving structural integrity. This study underscores the importance of integrating modern analytical techniques with traditional building practices to ensure the longevity and safety of masonry structures in the face of natural disasters

Keywords: Unreinforced Masonry Building, FEM, Pushover Analysis, Capacity Spectrum Method (CSM),

Table of Content

List of Figure

List of Table

CHAPTER 1: INTRODUCTION

1.1 General

Masonry involves constructing structures by assembling individual units that are bound together using mortar. Common materials for masonry include bricks, stones such as marble, granite, and limestone, as well as concrete blocks, glass blocks, and tiles. This method remains popular for residential and low-rise buildings due to its durability. However, factors like the quality of materials, the mortar, workmanship, and the arrangement of units significantly impact the overall longevity of masonry structures.

Brick and stone masonry offer advantages like durability, fire resistance, heat resistance, and aesthetic appeal, partly due to the easy availability of materials. While masonry is excellent at bearing compressive loads, it struggles with tensile loads, making masonry buildings inherently brittle. These structures are among the most susceptible to damage during strong earthquakes.

Due to their substantial mass, masonry buildings experience significant horizontal forces during seismic activity. Under these forces, they often develop numerous cracks from both compression and tension. The additional stresses caused by overturning moments during earthquakes can lead to structural failure.

Masonry structures can be broadly classified into Unreinforced Masonry (URM) and Reinforced Masonry (RM) with respect to structural engineering. Belo figure represents different type of masonry structures
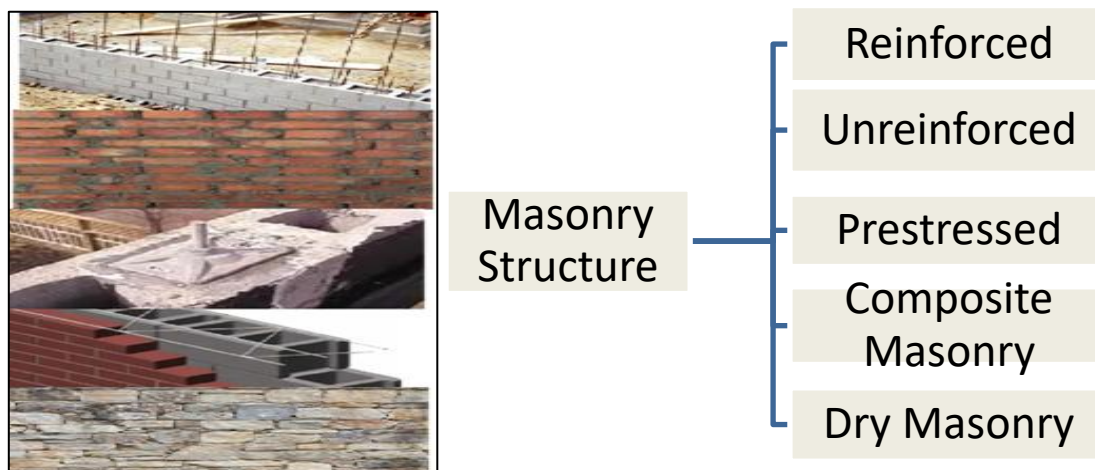
Figure 1. 1 Types of Masonry Structures Source: CMP stone

1.2 Seismic Adaptation in Jammu and Kashmir

- **Taq System:** Alternating timber and masonry walls with horizontal wooden beams embedded in the masonry. Timber bands distribute seismic forces evenly, providing ductility and flexibility. Commonly found in Srinagar and other parts of the Kashmir Valley

- **Dhajji-Dewari:** Timber-frame construction filled with masonry or bricks Acts like a shear wall, with timber absorbing seismic energy and reducing the risk of collapse.

- **Stone Masonry with Rubble Core:** Walls built with stone blocks and a rubble core without reinforcement. These are less resistant to lateral forces, making them dangerous in strong earthquakes (Jain, 2016)

Figure 1. 2 Seismic Adaptation in Jammu and Kashmir Source: (Jain, 2016)

1.3 Analytical Approach and Relevance

To capture the true behavior of URM buildings under seismic loads, simplified linear methods are often insufficient. Traditional analysis techniques do not adequately represent the nonlinear, brittle, and progressive failure characteristics of masonry. For a realistic evaluation of seismic performance, it is necessary to adopt more advanced methods that simulate actual damage mechanisms.

In this study, a Finite Element Method (FEM)–based approach is used to model and analyses URM structures. FEM allows for a detailed representation of material behavior, including

cracking, crushing, and inelastic deformation. The analysis is conducted using RFEM 6, a versatile structural engineering software platform capable of handling complex geometries and nonlinear simulations.

To evaluate performance, the study employs the Capacity Spectrum Method (CSM), a nonlinear static procedure that relates structural capacity with seismic demand. This approach provides valuable insights into the building's expected performance level during different intensities of ground shaking. The combination of FEM modelling and capacity-based assessment offers a comprehensive framework for understanding and improving the seismic resilience of URM buildings in high-risk areas.

Further details of the modelling process, parameters, and analysis strategy are provided in the methodology chapter.

1.4 Vulnerability of Unreinforced Masonry Buildings

Unreinforced masonry (URM) buildings are among the most seismically vulnerable construction types due to their structural characteristics and material limitations. These buildings are typically constructed using bricks, stones, or blocks laid in mortar, without the inclusion of reinforcement to resist tensile or shear stresses. While URM structures perform satisfactorily under vertical loads, their behavior under lateral forces—such as those induced during an earthquake—is far from reliable.

The primary reason for this vulnerability lies in the brittle nature of masonry. Unlike reinforced concrete or steel, masonry lacks the ductility required to absorb and dissipate seismic energy. During an earthquake, the lateral forces lead to cracking in walls, separation at joints, and in many cases, complete collapse of wall panels, especially in out-of-plane directions. Common failure mechanisms in URM structures include diagonal shear cracks, in-plane sliding, out-of-plane bending, corner dislocation, and roof-wall connection failures. Another factor contributing to the seismic vulnerability of URM buildings is their mass. These structures often have thick, heavy walls that attract high inertial forces during ground motion. Coupled with poor connection details and inadequate anchorage between walls and diaphragms (roofs/floors), this makes the entire system unstable when subjected to dynamic loads.

In many parts of India, including Jammu and Kashmir, URM buildings have been constructed over decades using traditional practices without formal engineering input. These structures often lack standardization in terms of materials, wall thickness, bond patterns, and

quality of workmanship, which further exacerbates their unpredictability under seismic loading.

The presence of irregular openings, unsymmetrical plans, and poor maintenance further deteriorate their performance during earthquakes. Historic data and post-earthquake reconnaissance studies have consistently shown that URM buildings suffer the most damage in seismic events, often resulting in significant loss of life and property.

Given their prevalence in seismic-prone regions such as Jammu and Kashmir, assessing the vulnerability of URM buildings is critical. A deeper understanding of their structural behavior enables engineers and decision-makers to prioritize retrofitting efforts, develop mitigation strategies, and enhance disaster preparedness at the community level.

1.5 Seismic Zonation and Risk Profile of Jammu & Kashmir

India is divided into four seismic zones—Zone II, III, IV, and V—based on the level of earthquake hazard. Zone II represents low risk, while Zone V indicates the highest level of seismic hazard. As per the classification in IS 1893 (Part 1):2016, **a significant portion of the Union Territory of Jammu & Kashmir falls under Zone V**, and the remaining under Zone IV. This implies that the region is subject to **high and very high seismic vulnerability**, respectively.

The location of Jammu & Kashmir on the **northwestern edge of the Indian tectonic plate** places it in proximity to the **active Himalayan thrust fault system**, which is a major source of seismic activity in the Indian subcontinent. Historical earthquakes, including the 2005 Muzaffarabad earthquake, have demonstrated the **devastating impact of seismic forces** on the region's-built environment.

The seismic zoning map of India, as shown in **Figure 1.3**, clearly highlights the high-risk categorization of Jammu & Kashmir. This classification is based on probabilistic seismic hazard assessments and past seismic activity records. The map plays a critical role in understanding the **urgency and need** for structural assessment and earthquake-resistant design, especially for vulnerable structures such as **unreinforced masonry (URM) buildings**, which are widespread in the region.
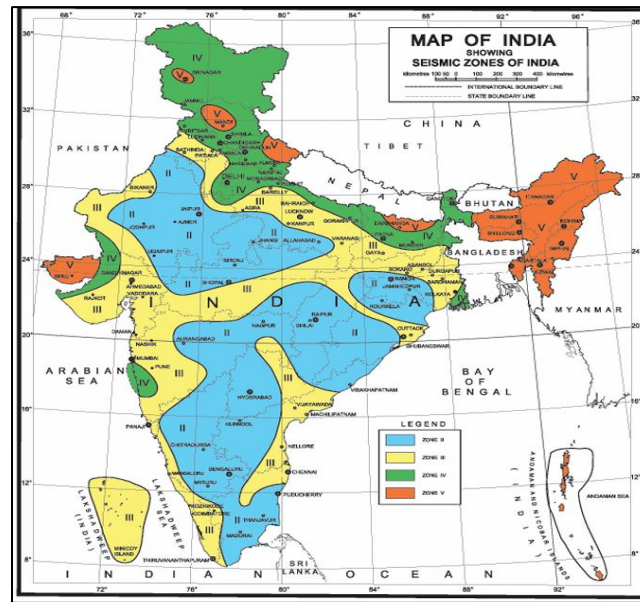
Figure 1.3 Seismic Zoning Map of India showing Jammu & Kashmir in Zones IV and V as per IS 1893 (Part 1):2016. This map highlights the high-to-very-high seismic risk level of the region.

1.6 Organization of Thesis

This thesis is organized into seven chapters, each structured to systematically present the research problem, background, methodology, and findings. A brief overview of each chapter is provided below:

- **Chapter1: Introduction**

  This chapter introduces the research background, highlighting the seismic vulnerability of unreinforced masonry (URM) buildings in Jammu and Kashmir. It presents the rationale, significance, analytical approach, and outlines the methodology and tools adopted, including a brief introduction to RFEM 6.

- **Chapter 2: Literature Review**

  This chapter provides a comprehensive review of past studies related to seismic performance assessment of URM structures, capacity spectrum methodology, fragility curve development, and the use of finite element methods in similar contexts. It helps in identifying research gaps and refining the scope of the current study.

- **Chapter 3: Methodology**

  This chapter explains the overall research methodology, including the step-by-step procedure followed for modeling, pushover analysis, and application of the Capacity

Spectrum Method. It also highlights the strategy adopted for data interpretation and result generation.

- **Chapter 4: Finite Element Modelling**

  This chapter details the modeling of URM buildings using RFEM 6. It discusses the structural configuration, element definition, loading patterns, boundary conditions, and the nonlinear analysis carried out to obtain the pushover curve.

- **Chapter 5: Results And Discussion of Modal and Pushover Analyses**

  This chapter presents the results of modal and pushover analyses performed on URM models. It highlights the dynamic behaviour, structural capacity, and performance point evaluation using the Capacity Spectrum Method. Modal analysis provides natural periods and mode shapes, helping assess seismic sensitivity. Pushover curves are analysed to identify strength, stiffness degradation, and displacement capacity. A comparative discussion among models is included to understand relative vulnerability.

- **Chapter 6: Vulnerability Assessment using Fragility Curves**

  In this chapter, the seismic capacity of the buildings is evaluated through fragility analysis. Fragility curves are developed using results from the capacity spectrum approach, helping to quantify the probability of damage at various seismic intensity levels.

- **Chapter 7: Summary and Conclusions**

  This final chapter summarizes the key findings of the study, presents conclusions based on the analysis, and offers recommendations for future work. The practical implications of the research in terms of seismic risk mitigation for URM buildings in Jammu and Kashmir are also discussed

CHAPTER 2: LITERATURE REVIEW

2.1 Literature review of research paper

Lipika Halder, Sekhar Chandra Dutta, Pranoy Debnath, Richi Prasad Sharma "Seismic Vulnerability assessment of low-rise unreinforced Masonry Buildings in Northeast India Considering Variability of Material Properties" Asian Journal of Civil Engineering (Springer) 2021.

Unreinforced masonry buildings are common in India in this research paper the author used Equivalent Frame Modelling (EFM) to simulate global behaviour while addressing computational constraints.

The study contributes to assess Seismic Vulnerability of URM Buildings using Fragility analysis.

Total 60 buildings models have been developed and nonlinear static analysis is performed to obtain cumulative distribution function (cdf) of displacement demand and pdf of damage states.

They have derived fragility curves Using FEMA 440 methods and IS 1893 (2016) guidelines for seismic demand assessment (Lipika Halder, 2021)

Yogendra Singh, Dominik H. Lang, JSR Prasad and Rajesh Deoliya "An Analytical Study on the Seismic Vulnerability of Masonry Buildings in India", Journal of Earthquake Engineering (Taylor and Francis) 2012.

In this article two Equivalent frame models have been presented which can be easily implemented in available software and can simulate the interaction of axial force with lateral action in shear and rocking. • Vulnerability functions are estimated using the obtained Capacity curves. • Damage probability Matrices (DPMs) are obtained using the approximate PGA-intensity correlation relationship as per Indian seismic building code. • Damage predicted by the analytical simulation is slightly higher than the predicted by the PSI scale, but it is lower than that observed during the 2001 Bhuj Earthquake. • The possible reason

for predicting lower damage is ignoring out-of-plane failure of masonry walls (Singh, 2013)

Amir Hossein Shabani, Mahdi Kioumarsi, Maria Zucconi "State of the art of simplified analytical methods for seismic vulnerability assessment of unreinforced masonry buildings", Engineering Structures (Elsevier) 2021.

In this article the simplified methods are categorized in three groups: Analytical, Empirical and Hybrid methods. The study simplified analytical methods for the seismic vulnerability assessment of unreinforced masonry (URM) buildings were reviewed, starting with their classification into three main groups. Collapse mechanism-based, Capacity Spectrum based, and fully displacement based (Shabani, 2021)

Nouman Khattak, Hossein Derakshan Tiago Miguel Ferreira et.al. "Seismic Vulnerability assessment of pre-1945 unreinforced masonry buildings located in Queensland, Australia, using an index-based approach", Structures (Elsevier) 2021.

In this study it's finding indicates that many of assessed buildings are potentially vulnerable to earthquakes of low to moderate intensities, necessitating, therefore, further investigation using more detailed tools. • A total of 363 URM buildings across seven towns of QLD were assessed using existing data gathered through field surveys. The findings are analyzed and compared to previous vulnerability studies on similar building typologies in Australia and are presented through maps created using an open Geographical Information System (GIS) tool. The insights generated in this research can serve as a valuable resource for identifying critical buildings and proposing conservation or retrofitting plans. (Khattak, 2024)

Turgay Cos gun, Oguz Uzdil, Baris Sayin, Kamil Keren Zengin "Seismic vulnerability assessment of masonry structure and an FRP-strengthening proposal", Case Studies in Construction Materials (Elsevier) 2022.

This paper presents an approach to seismic performance evaluation for masonry structures using linear, nonlinear, and Kinematic analysis which has been used frequently in recent years to evaluate the earthquake safety of masonry buildings. Briefly, this method includes, identifying possible collapse mechanisms, ii. determining lateral forces that trigger a collapse mechanism and the lateral peak ground acceleration required for this lateral force, iii. comparing the required lateral peak ground acceleration with the capacity of the structure and determining the possible mechanism the performance of the building was analyzed using

the assumptions and the parameters given in the TBEC 2018 code. A linear elastic analysis was performed for the building exposed to earthquake loads. Accordingly, the structural strength of the building was found to be insufficient. Therefore, a fiber-reinforced polymer -strengthened design proposal was presented. (Cosgun, 2022)

Miguel Gonçalves, Madalena Ponte and Rita Bento "Seismic Assessment of Existing Masonry Buildings Using Damage Mechanics", Buildings (MDPI) 2024.

In this paper a nonlinear static analysis is undertaken using the commercial software ABAQUS standard in which masonry structures are modelled using damage mechanics. To validate the chosen input parameters, this study compares two different approaches for static nonlinear modelling, the Finite Element Method (FEM) and the Equivalent Frame Method (EFM), for a simple masonry building. The two methods are compared using the guidelines from Part 3 of Eurocode 8. The results are also compared in terms of capacity curves and damage distributions for the simple case study of a masonry building created to compare numerical methods. Subsequently, nonlinear pushover analyses with ABAQUS (FEM) were performed on the North Tower of Monserrate Palace, Portugal, in which the material parameters were calibrated by considering the results of characterization tests conducted in-situ. (Gonçalves, 2024)

Yohei Endo, Lucapela, and Pere Roca "Review of Different Pushover Analysis Methods Applied to Masonry Buildings and Comparison with Nonlinear Dynamic Analysis", Journal of Earthquake Engineering (Taylor & Francis) 2016.

Nonlinear seismic analysis methods, such as invariant pushover analysis (IPA), adaptive pushover analysis (APA), and nonlinear dynamic analysis (NDA), are extensively used for evaluating masonry structures under seismic loading. A review of these methods highlights their application to simplified case studies, including a four-wall masonry building without rigid diaphragms and a two-wall system with a cross-vault, representing common historical constructions. The study examines how lateral force distributions influence IPA results, compares them with APA outcomes, and benchmarks all approaches against NDA results using both artificial and natural accelerograms with varying intensities. This comparison elucidates the advantages, reliability, and limitations of each method for masonry seismic analysis. (Endo, 2017)

Abide Aşıkoğlua, Graça Vasconcelosa, Paulo B. Lourençoa, Bartolomeo Pantò

"Pushover analysis of unreinforced irregular masonry buildings: Lesson from different modelling approaches", Engineering Structures (Elsevier) 20220.

This study evaluates the seismic performance of unreinforced masonry (URM) buildings with plan and elevation irregularities through nonlinear static analyses. Utilizing a continuum model and simplified approaches like spring-based macro-elements and equivalent frame models, the research compares numerical results against experimental data from shaking table tests. It highlights critical factors such as torsional effects, elastic property adjustments, and failure modes, emphasizing their influence on the reliability of simplified methods. While continuum models align closely with experimental results, simplified models show variability, raising concerns about their reliability for irregular masonry buildings. The findings underline the need for accurate methodologies to account for irregularities in seismic assessments and design practices. (Abide Aşıkoğlua, 2020)

GR. G. Panels "Seismic Assessment of Existing Masonry Buildings Using Damage Mechanics, Journal of Earthquake Engineering (Taylor and Francis) 2006.

In this paper methodologies for analyzing unreinforced masonry (URM) structures, highlighting the evolution of simplified and computationally efficient approaches. It draws parallels with the equivalent frame models previously developed by Magnes and Della Fontana (1998), emphasizing the use of point hinge models to simulate the nonlinear behavior of URM structures with openings. Key prior advancements include the adoption of analytical models for flexural response, utilizing concepts such as the parabolic compression stress block and Mohr-Coulomb failure criterion for shear strength assessment. While sophisticated finite element models offer detailed crack pattern predictions, the literature underscores the utility of simplified equivalent frame approaches in practical engineering applications, especially for rehabilitation guidelines (Penelis, 2006)

Faisal Mehraj Wani, Ruthviz Kodali, Vanga Amulya Reddy et. al. "Finite element analysis of unreinforced masonry walls with different bond patterns", Sustainable Engineering and Innovation (2023)

In this paper methodologies for analyzing unreinforced masonry (URM) structures, highlighting the evolution of simplified and computationally efficient approaches. It draws parallels with the equivalent frame models previously developed by Magnes and Della Fontana (1998), emphasizing the use of point hinge models to simulate the nonlinear

behavior of URM structures with openings. Key prior advancements include the adoption of analytical models for flexural response, utilizing concepts such as the parabolic compression stress block and Mohr-Coulomb failure criterion for shear strength assessment. While sophisticated finite element models offer detailed crack pattern predictions, the literature underscores the utility of simplified equivalent frame approaches in practical engineering applications, especially for rehabilitation guidelines. (Wani, 2023)

2.2 Need of Study

2.2.1 Seismic Vulnerability

- Many regions in India, including the Himalayan belt (Zones IV and V), Northeast, and parts of Gujarat, experience high seismic activity. URM structures, being brittle and unable to withstand lateral loads, are prone to catastrophic collapse during earthquakes, leading to significant loss of life and property.

2.2.2 Lack of Structural Integrity:

- Proper bond between masonry units.
- Seismic-resistant features like lintel bands or shear reinforcements.

- This results in weak connections and poor load distribution, making them unsafe under dynamic loads

2.2.3 Need for Retrofitting and Disaster Mitigation

- Many existing URM structures fail to meet modern seismic design codes. Studying these buildings helps in:

- Identifying weaknesses in construction.

- Developing cost-effective retrofitting techniques.

- Enhancing resilience to future earthquakes

2.3 Objective

- To Design and Analyze symmetric unreinforced masonry structures using FEM Software

- Conducting a nonlinear static Pushover analysis of selected URM Building using IS

located in the Jammu & Kashmir, India.

- Seismic Vulnerability assessment of selected URM building using Capacity Spectrum-Based Method

2.4 Scope of Work

- To Design and Analyse the existing URM building using Dlubal Rfem-6 software by FEM approach.
- Conduct Non-Linear static pushover analysis of Selected URM Building located in Jammu &Kashmir Using FEM approach with respect to Indian standards.
- Derive the seismic fragility curves for the selected URM building Using Capacity Spectrum Based method.

2.5 IS Codes of practice for Masonry structures

➢ **IS 4326: 2013**

Title: Earthquake Resistant Design and Construction of Buildings - Code of Practice

Scope: Provides guidelines for designing and constructing earthquake-resistant buildings, including considerations for masonry structures. It outlines the principles of ductility, strength, and construction techniques to minimize earthquake damage.

➢ **IS 13828: 1993**

Title: Guidelines for Improving Earthquake Resistance of Low Strength Masonry Buildings

Scope: Focuses on retrofitting and strengthening low-strength masonry buildings to improve their earthquake resistance.

➢ **IS 1893: Part 1: 2016**

Title: Criteria for Earthquake Resistant Design of Structures - Part 1: General Provisions and Buildings

Scope: Lays down seismic design criteria and zones for all types of structures, including masonry buildings.

➢ **IS 1905: 1987**

Title: Code of Practice for Structural Use of Unreinforced Masonry

Scope: Specifies design and construction guidelines for unreinforced masonry structures, addressing issues like load distribution and stability.

➢ **IS 1597 (Parts 1 & 2)**

Title: Construction of Stone Masonry - Code of Practice

Scope: Covers the design and construction of rubble and ashlar stone masonry.

➢ **IS 2212: 1991**

Title: Brickwork - Code of Practice

Scope: Focuses on good construction practices for brick masonry, including material selection, bonding, and structural consideration

CAPTER 3 METHODOLOGY

3.1 Finite element analysis

Finite element analysis (FEA) is a numerical method that addresses complex problems involving various shapes, boundary conditions, and loads. While the results obtained through FEA are approximations, the method's versatility and adaptability as an analytical tool have garnered significant attention in the engineering field. The primary requirement for utilizing FEA is a computer, and recent advancements in computer hardware technology, along with a decrease in computer costs, have further propelled the method's popularity.

Several well-known FEA software packages are now available in the market, including STAAD-PRO, GT-STRUDL, ABAQUS, and ANSYS. These tools enable engineers to analyze a wide range of complex structures.

Originally, the FEA method was developed for stress analysis in aircraft design, evolving from the matrix method of structural analysis. Nowadays, FEA is employed in various applications, including fluid flow analysis, heat transfer, and the study of electric and magnetic fields.

Civil engineers frequently utilize this technique to analyze structural members, frames, shells, folded plates, foundations, and the seepage of fluids through porous media. FEA is adept at addressing both static and dynamic problems.

Numerous engineering challenges involve nonlinear stress-strain relationships and strain-displacement interactions. As computer capabilities continue to expand, researchers are able to analyze structures more comprehensively, incorporating real stress-strain curves and geometric changes resulting from applied loads.

3.2 SEISMIC EVALUATION METHODS

To comprehensively assess a building's seismic vulnerability, it is essential to adopt a structured approach that incorporates multiple analysis methods. Recommended methods include:

1. Linear Static Analysis (Equivalent Static Method)
2. Linear Dynamic Analysis (Response Spectrum Method)
3. Nonlinear Static Analysis (Pushover Analysis)

For a thorough evaluation, it is advisable to conduct these analyses in sequence. Although a more advanced technique, the nonlinear dynamic time-history analysis, is available, it is generally not recommended for standard buildings due to its complexity and the time it requires.

The primary aim of both linear static and linear dynamic analyses, as specified in Indian Standard IS 1893:2002, is to ascertain the demand-to-capacity ratios of structural components, thereby ensuring adherence to seismic design regulations. Either of these methods can be utilized to estimate the anticipated seismic forces acting on the lateral load-resisting elements. A detailed discussion of the nonlinear static pushover analysis will be presented in the following section.

3.2.1 Equivalent Static Method (Standards, 2016)

In the Equivalent Static Method, the seismic force corresponding to the Design Basis Earthquake (DBE) is applied statically to the structure. The equivalent lateral forces at each story level are considered at the respective floor levels.

The total seismic base shear (V) is determined as per Clause 7.6 of IS 1893:2016. This calculation ensures that the applied forces accurately represent the earthquake-induced effects on the structure, enabling a proper evaluation of seismic performance and compliance with design standards.

$$V_B = A_h . w$$

where,

A_h= design horizontal acceleration coefficient value as per **6.4.2**, using approximate

fundamental natural period T_a as per **7.6.2** along the considered direction of shaking; and W= seismic weight of building as per **7.4**

$$A_h = \left(\frac{Z}{2}\right)\left(\frac{I}{R}\right)\left(\frac{Sa}{g}\right)$$

In the context of seismic design, the following parameters are defined:

W: seismic weight of the building

Z: zone factor

I: importance factor

R: response reduction factor

Sa/g: spectral acceleration coefficient, which is determined based on specific criteria corresponding to an approximate time period (T_a) which is given by

$$\text{a)} \quad Ta = \begin{cases} 0.075h^{0.75} \\ 0.080h^{0.75} \\ 0.085h^{0.75} \end{cases}$$

  i.   For RC MRF building
  ii.   For RC-Steel Composite MRF building
  iii.   For steel MRF building

  b) Buildings with RC structural walls

$$T_a = \frac{0.075h^{0.75}}{\sqrt{Aw}} \geq \frac{0.09h}{\sqrt{d}}$$

  c) All other buildings:

$$Ta = \frac{0.09h}{\sqrt{d}}$$

The base dimension of the building at the plinth level, in the direction of lateral forces, is denoted as 'd' (in meters), while the height of the building from the support is represented as 'h' (in meters).

The response spectrum functions can be calculated as follow:

  d) For use in equivalent static method

$$\frac{Sa}{g} = \begin{cases} \text{For rocky or hard soil sites} \begin{cases} 2.5 & 0 < T < 0.40\ s \\ \dfrac{1}{T} & 0.40\ s < T < 4.00\ s \\ 0.25 & T > 4.00\ \ s \end{cases} \\[3em] \text{For Medium stiff soil sites} \begin{cases} 2.5 & 0 < T < 0.55\ s \\ \dfrac{1.3}{T} & 0.55\ s < T < 4.00\ s \\ 0.34 & T > 4.00\ s \end{cases} \\[3em] \text{For soft soil sites} \begin{cases} 2.5 & 0 < T < 0.67\ s \\ \dfrac{1.67}{T} & 0.67\ s < T < 4.00\ s \\ 0.42 & T.4.00\ s \end{cases} \end{cases}$$

e) For use in response spectrum method

$$\frac{Sa}{g} = \begin{cases} \text{For rocky or hard soil sites} \begin{cases} 1 + 15T & T < 0.10\ s \\ 2.5 & 0.10s < T < 0.40\ s \\ \dfrac{1}{T} & 0.40\ s < T < 4.00\ s \\ 0.25 & T > 4.00\ \ s \end{cases} \\[4em] \text{For Medium stiff soil sites} \begin{cases} 1.15T & T < 0.10s \\ 2.5 & 0.10\ s < T < 0.55\ s \\ \dfrac{1.36}{T} & 0.55\ s < T < 4.00\ s \\ 0.34 & T > 4.00\ s \end{cases} \\[4em] \text{For soft soil sites} \begin{cases} 1 + 15T & T < 0.10\ s \\ 2.5 & 0.10\ s < T < 0.67\ s \\ \dfrac{1.67}{T} & 0.67\ s < T < 4.00\ s \\ 0.42 & T > 4.00\ s \end{cases} \end{cases}$$

The design base shear is to be distributed along the height of building as per Clause 7.7.1 of (Standards, 2016)
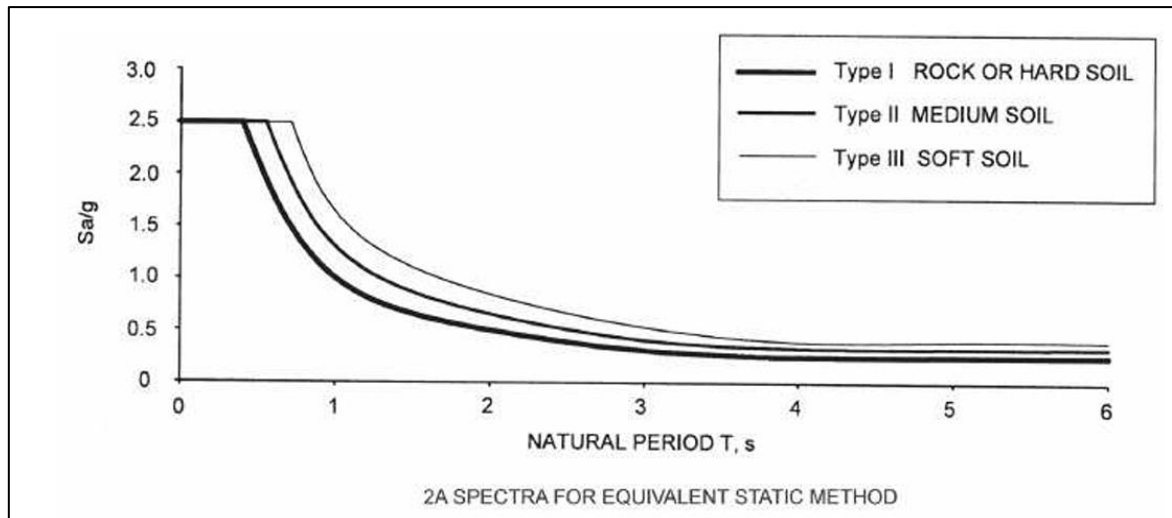
Figure 3. 1 Response spectrum as per IS 1893:2016
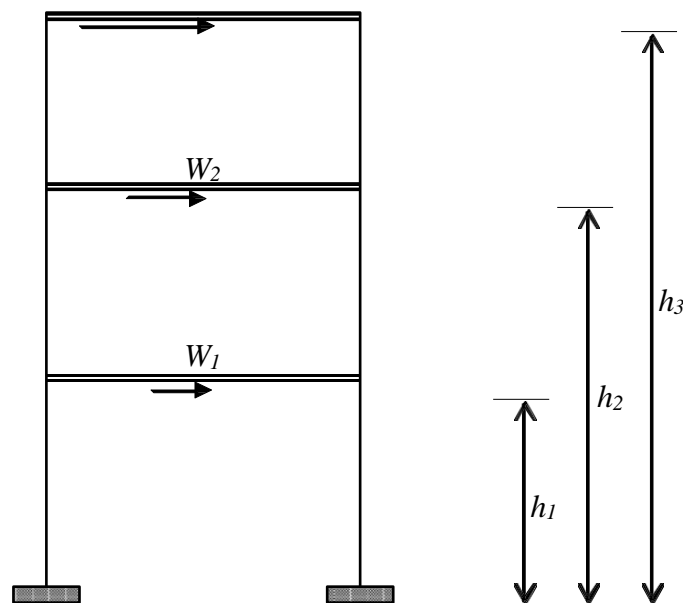
Figure 3. 2 Lateral load distribution

Building model under seismic load

The design base shear (VB) computed shall be distributed along the height of the building and in plan at each floor level as below

$$Q_i = \left(\frac{W_i h_i^{\,2}}{\sum\limits_{j=1}^{n} W_j h_j^{\,2}} \right) VB$$

Where;

Qi = design lateral force at floor i;
W_i = Seismic weight of floor i;

h_i = Height of floor measured from base,

n = Number of stories in the building equal to the number of levels at which masses are located

3.2.2 Pushover Analysis

Pushover analysis is a method of nonlinear static analysis utilized in structural engineering to evaluate the seismic performance of buildings. This approach examines how a structure reacts to gradually increasing lateral forces, such as those produced by earthquakes, until it either fails or reaches a specified performance limit. As these lateral forces rise, certain elements of the structure may undergo plastic deformations. The analysis effectively illustrates how the structure redistributes loads and continues to deform under stress. Loads are applied incrementally until the structure reaches a target displacement or ultimately fails. This target displacement usually indicates a threshold where significant damage occurs, while the structure remains stable. The outcomes of a pushover analysis are represented by a capacity curve, also referred to as a pushover curve, which shows the relationship between the building's base shear (the total lateral force at the base) and the roof displacement (the horizontal movement of the roof).
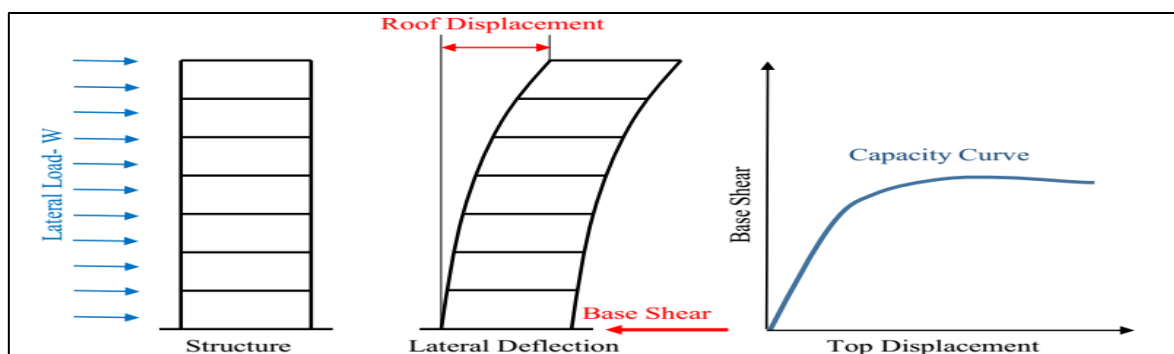
Figure 3.3 Systematic diagram of pushover analysis

3.3 Seismic Vulnerability assessment methods

Seismic vulnerability refers to the susceptibility of a structure to damage or failure when subjected to earthquake forces. It depends on factors such as structural configuration, material properties, foundation conditions, and construction quality. High seismic vulnerability means a structure is more likely to experience significant damage during an earthquake.
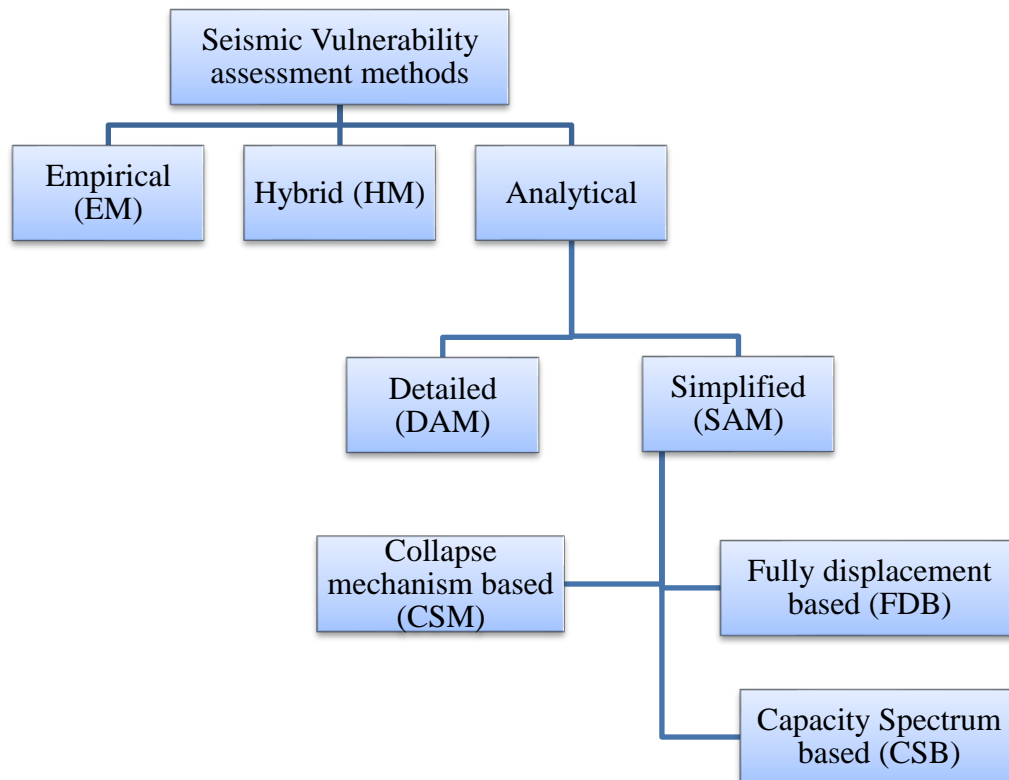
Figure 3.4 Seismic Vulnerability assessment methods

3.3.1 Capacity Spectrum Method (ATC-40) (Council, 1996)

The Capacity Spectrum Method (CSM) is a performance-based seismic assessment technique used to evaluate the response of structures subjected to earthquake forces. It is based on the idea that the maximum inelastic displacement of a nonlinear structure can be approximated using the maximum displacement of an equivalent linear system with adjusted properties.

The maximum inelastic displacement of a nonlinear single-degree-of-freedom (SDOF) system can be estimated using the maximum displacement of an equivalent linear elastic SDOF system with adjusted period and damping.

In this approach, the effective period and damping are determined using estimated ductility values.

The method utilizes the pushover curve, which is transformed into an Acceleration-Displacement Response Spectrum (ADRS) format. This transformation is achieved through a straightforward conversion process that relies on the dynamic characteristics of the structure.

The capacity spectrum represents the structural capacity in ADRS format, while the demand spectrum characterizes the seismic ground motion in the same format. The intersection of these two spectra provides insight into the expected seismic performance of the structure, helping engineers assess its response under earthquake loading.
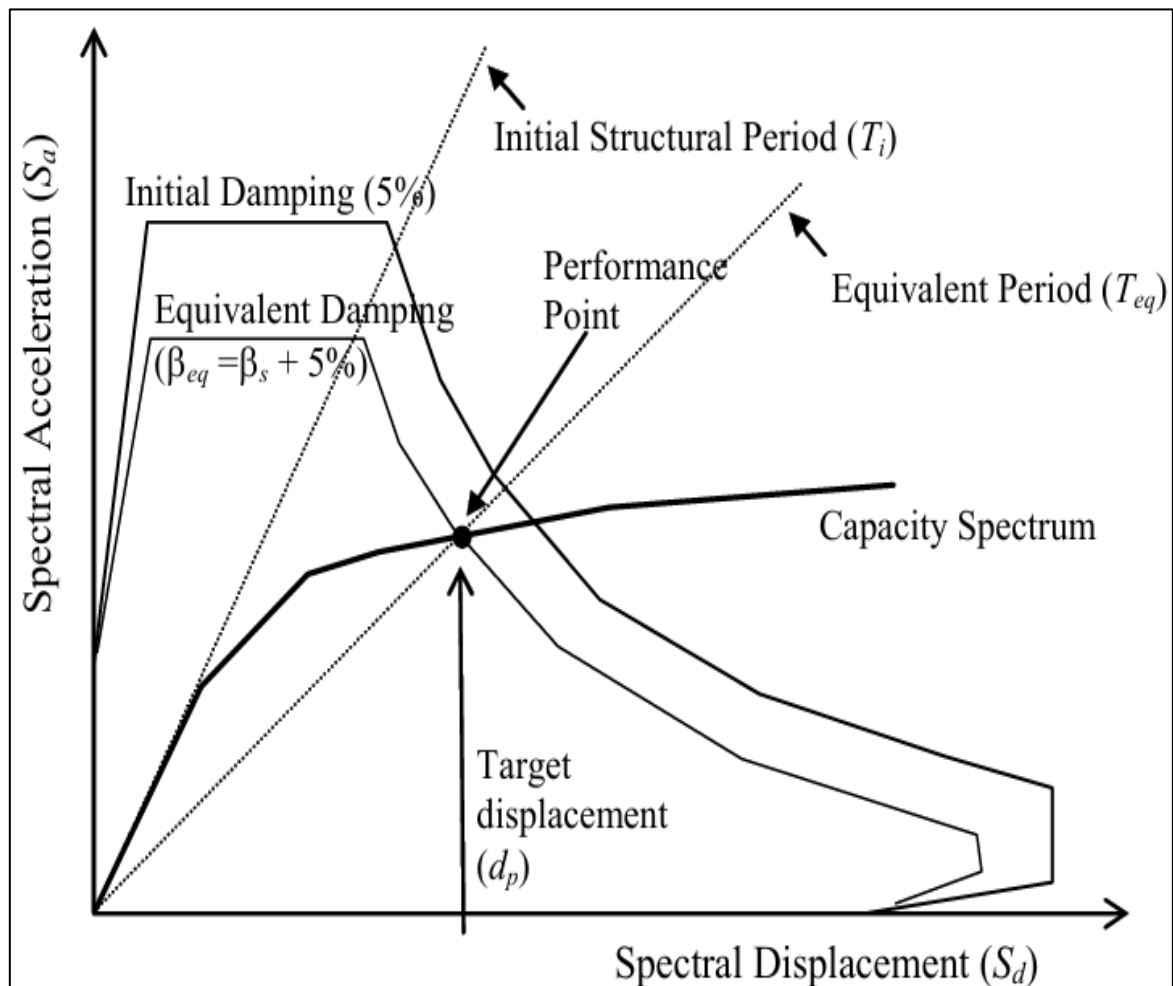
Figure 3. 5 Schematic representation of Capacity Spectrum Method (ATC 40)

3.4 Summary:

This chapter outlines the seismic evaluation methods used for assessing the vulnerability of unreinforced masonry buildings. It explains the application of Finite Element Modelling (FEM) for detailed 3D modelling and analysis using RFEM 6 software, focusing on modal, response spectrum, and pushover analyses. The chapter also discusses the Equivalent Static Method for calculating seismic forces in a simplified manner. Additionally, it covers two seismic vulnerability assessment methods: the Capacity Spectrum Method (ATC-40), which evaluates a building's capacity to resist seismic forces, and the N2 Method (Eurocode 8), providing a simplified approach to estimate seismic demand and capacity. These methods collectively form the basis for understanding and assessing the seismic performance of the buildings.

CHAPTER 4: FINITE ELEMENT MODELLING

4.1 Introduction

This chapter commences with a detailed examination of the geometric characteristics of the existing masonry building utilized in the study. The second section presents the pushover analyses for both single-story and double-story structures, along with a comparative study of the lateral behavior of various masonry types, analyzed through finite element method (FEM) analysis. Following the pushover analysis, which considers both dead and seismic loads, fragility curves are generated to assess seismic vulnerability.

4.2 Overview of RFEM 6 and Masonry Design Add-on (GmbH, 2025)

RFEM 6 is a comprehensive finite element analysis (FEA) software developed by Dlubal Software, designed for the structural analysis and design of planar and spatial systems, including plates, walls, shells, and members. Its modular architecture allows for the integration of various add-ons to extend its capabilities for specific structural materials and design standards

One such extension is the **Masonry Design Add-on**, which is shown in **4.3 Figure** which enables the modelling and analysis of masonry structures using the finite element method. This add-on incorporates specialized material models that simulate the nonlinear behaviour of masonry, accounting for its unique characteristics such as anisotropy and brittle failure modes. It allows for the design of masonry walls and structures by considering factors like compression and shear stresses, and it supports the assessment of different failure mechanisms inherent to masonry materials.

The integration of the Masonry Design Add-on within RFEM 6 facilitates a more accurate and detailed analysis of unreinforced masonry buildings, particularly in seismic vulnerability assessments. By leveraging this tool, engineers can model complex masonry geometries, apply relevant loads, and evaluate the structural performance under various conditions, thereby enhancing the reliability of the design and assessment process.
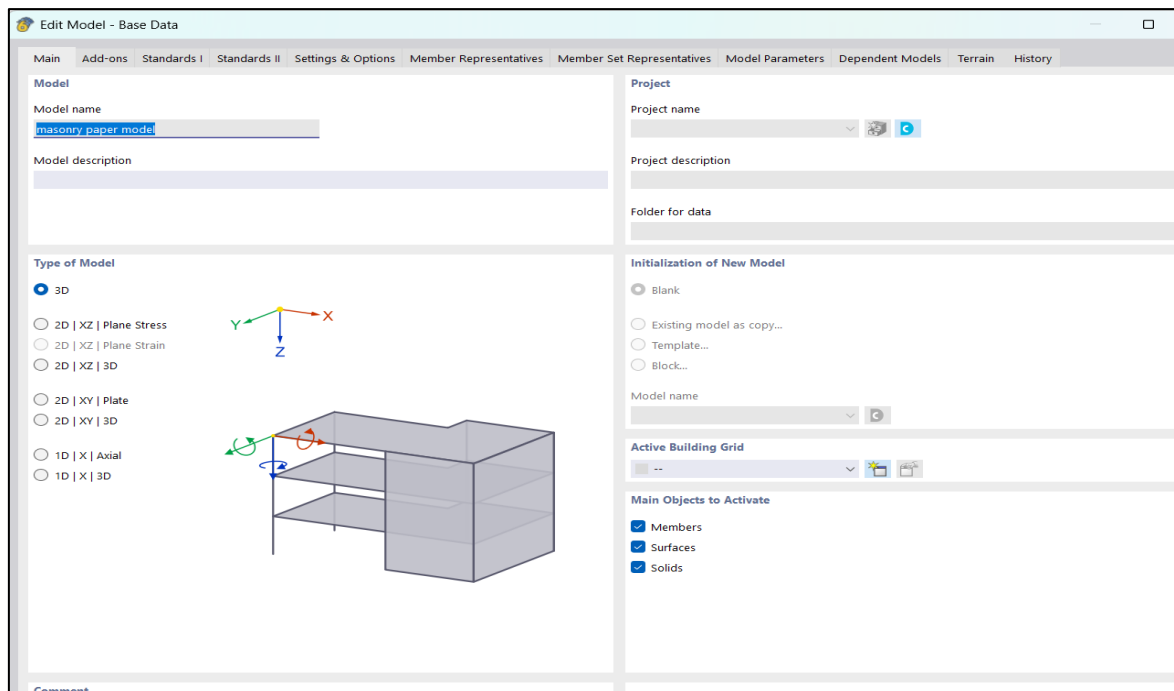
Figure 4.1 General Setup

This image shows the base data setup in RFEM 6. The selected options include Nonlinear Material Behavior, Modal Analysis, and Pushover Analysis under the analysis add-ons, along with Masonry Design under the design add-on.
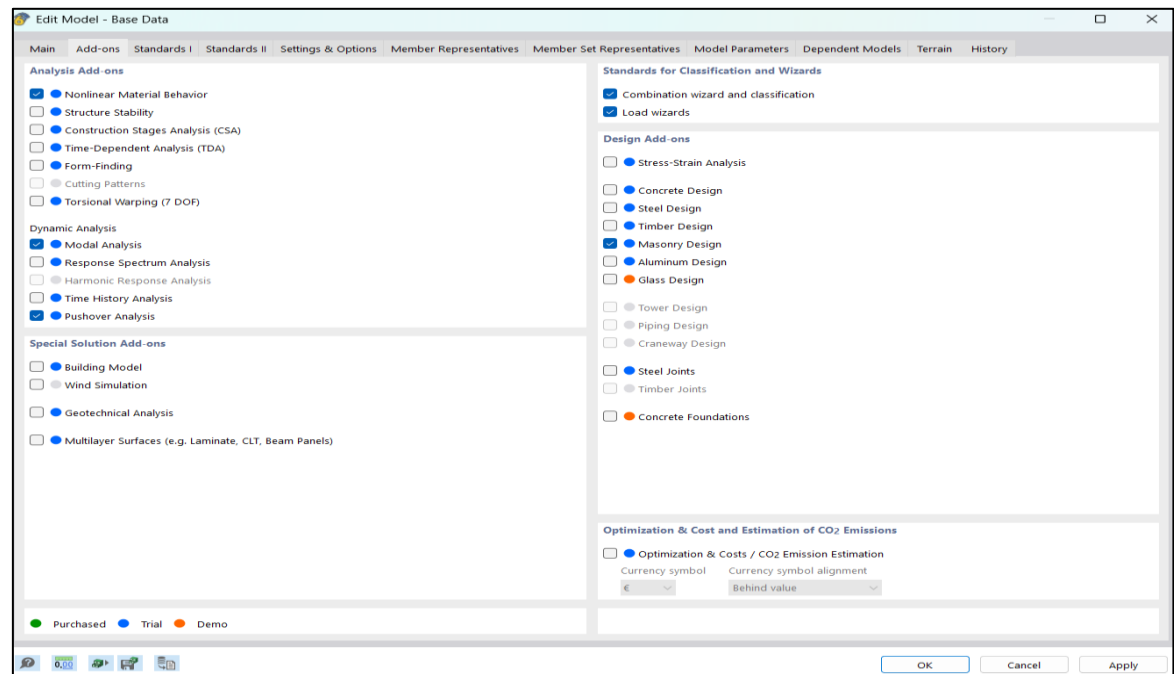
Figure 4.2 Add on related to the research

4.2.1 Modeling Workflow
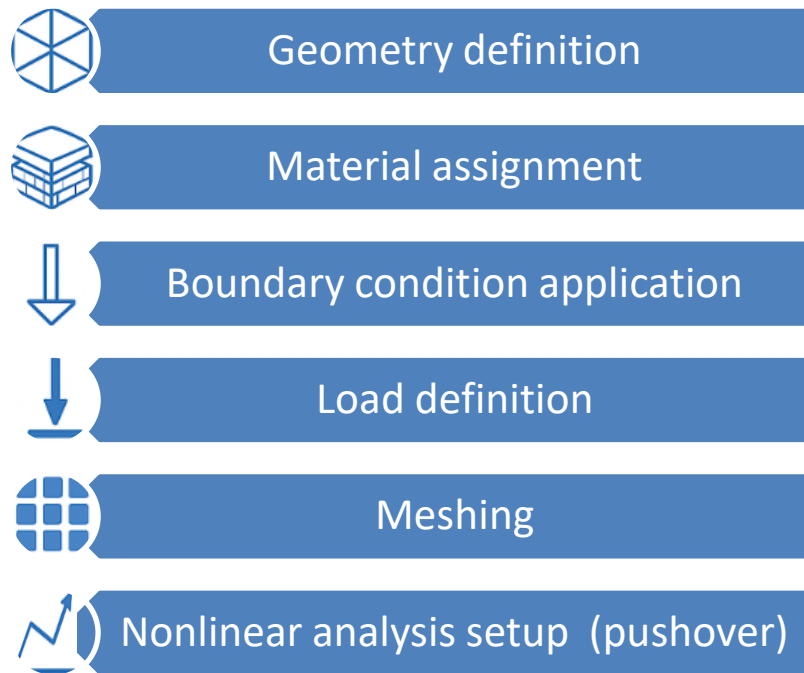
Figure 4.3 Modeling work flow

4.3 Modeling Strategy

For the current study, a macro-modelling approach is employed. In this method, masonry is treated as a homogenized material with averaged properties, rather than modelling individual bricks and mortar joints. This simplification is computationally efficient and is appropriate for global behaviour analysis, particularly when the objective is to assess overall structural performance under seismic loading.

Modelling Assumptions:

- The base of the walls is considered rigidly supported (fixed boundary conditions).
- The structure lacks a rigid diaphragm; floor behaviour is assumed to be flexible.
- The model includes self-weight and imposed live loads.
- No reinforcements are considered; the simulation represents pure unreinforced masonry behaviour.
- Masonry tensile strength is neglected, in line with standard practice for URM seismic modelling.

4.4 Geometric Modelling of Masonry Building

A comprehensive pushover analysis of the two-story unreinforced masonry structure, one story URM and two models of bathrooms which includes door and window openings, has been conducted using finite element modeling. The wall modeling follows the guidelines mentioned in the book. The plan A, B, C, D, represents the model which are illustrated in Fig. 4.3. the figure represents the drafted plan of structure in AutoCAD and RFEM 6. The plan is asymmetrical, and the varying sizes of the doors and windows affect the wall thickness, which measures 0.23 m for the outer wall and 0.115 m for the inner wall. For plan (A) there are different irregularities are provided such as wall height increased opening size changed etc.

Figure 4.3 Represents the figures of Layout pf Plan

4.4.1 Plan Dimensions and Wall Thickness

The Plan is taken as a real-life structure with asymmetric dimensions also one plan is taken

from Research paper to be a square plan structure, with dimensions 6.096 m * 6.096 m, 5.25 *3.050. The choice of a symmetric plan helps eliminate torsional irregularities during seismic analysis, thereby simplifying interpretation of the lateral response. All walls are modelled with a uniform thickness of 230 mm, and 240 mm consistent with standard load-bearing masonry practices in Indian construction.

4.4.2 Wall Height and Openings

The height of the masonry walls is taken as 3.35 m, for Plan A, D and 3.0 m for plan B, C. providing a typical single-story room proportion. Below table represents the height dimension of the openings and the heigh of wall for all the four plans.

For simplification and to focus on wall behaviour, no openings (windows or doors) are introduced in the model tested as D. This assumption allows the study to isolate the structural response of solid URM walls under seismic loading.
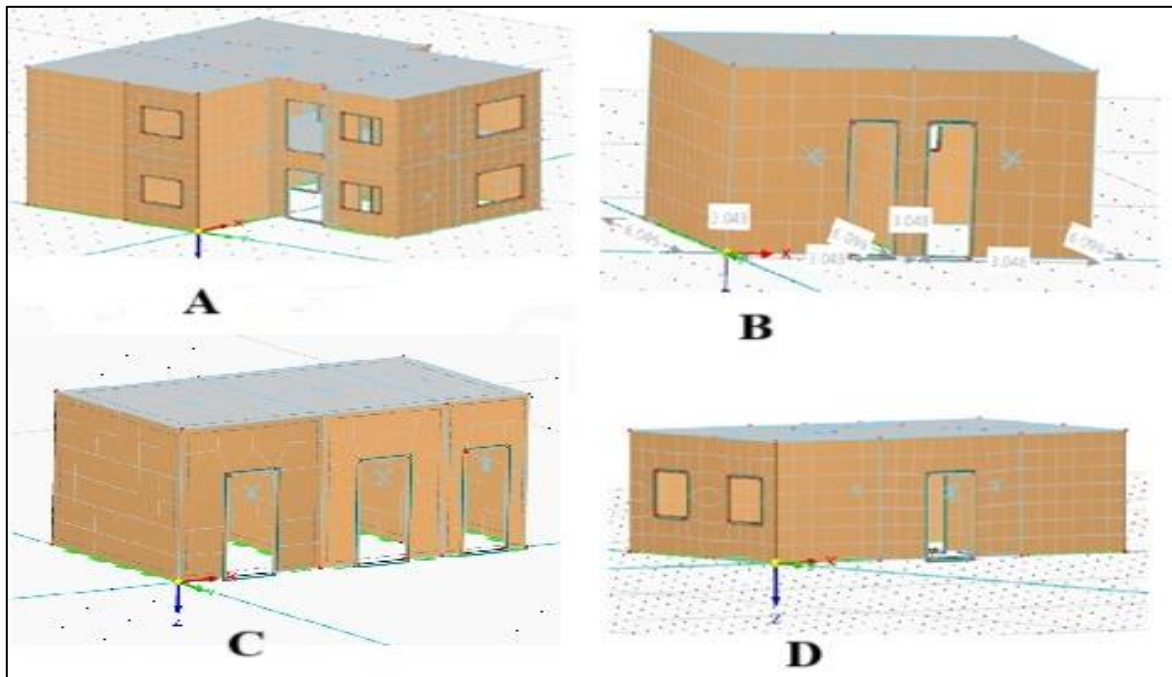
Figure 4.4 3D-View of Model

4.4.3 Structural System

The structural configuration does not include any reinforced concrete elements, frames, but only it includes reinforced slabs. The entire load-resisting system comprises vertical masonry walls only.

4.4.4 Idealization in RFEM

In RFEM 6, the walls are modelled as vertical surface elements. These surfaces are defined by their corner nodes, thickness, and material properties. No beam or column elements are introduced, and each wall segment acts as a planar vertical load-bearing unit.

This geometric setup enables a controlled environment for evaluating the seismic vulnerability of URM structures, especially under nonlinear static (pushover) loading conditions. It serves as the base case for further comparative assessments involving fragility analysis and capacity curve derivation.

4.5 Material Properties

In this study, unreinforced masonry (URM) walls were modelled using material properties derived in accordance with relevant Indian Standards, particularly IS 1905:1987 (Code of Practice for Structural Use of Unreinforced Masonry) and IS 3495 series (Methods of tests of burnt clay building bricks). The structural modelling was performed using RFEM 6, incorporating these parameters into the Masonry Design add-on.

Material Definition

The properties for URM were defined using custom material input in RFEM 6, based on the typical characteristics of burnt clay bricks and cement mortar:
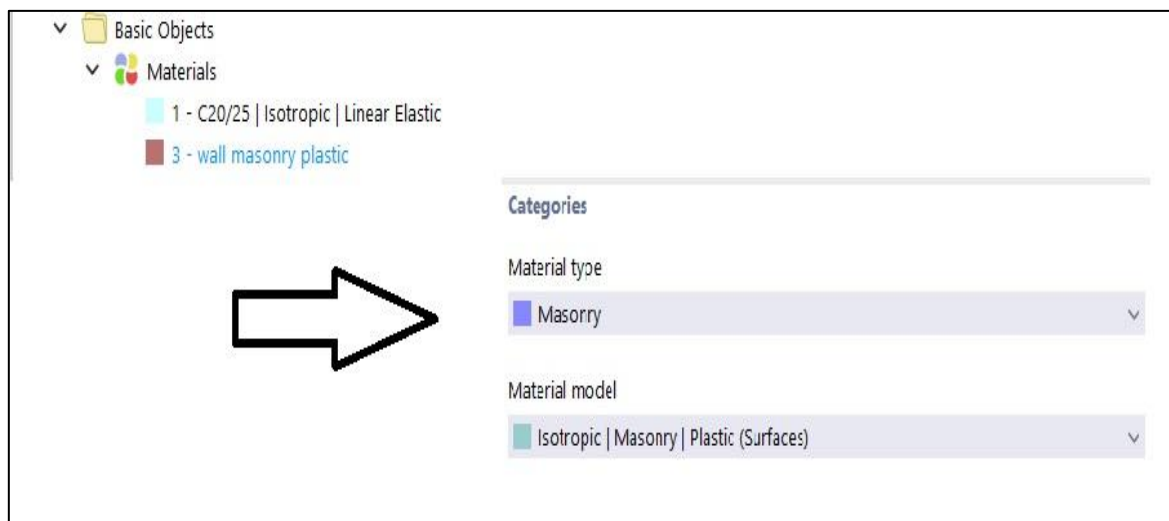
Figure 4.5 Represents the material properties selection in RFEM-6

The properties are defined as 2nd class burnt clay brick and the compressive strength and modulus of elasticity taken from the excel sheet which is presented below
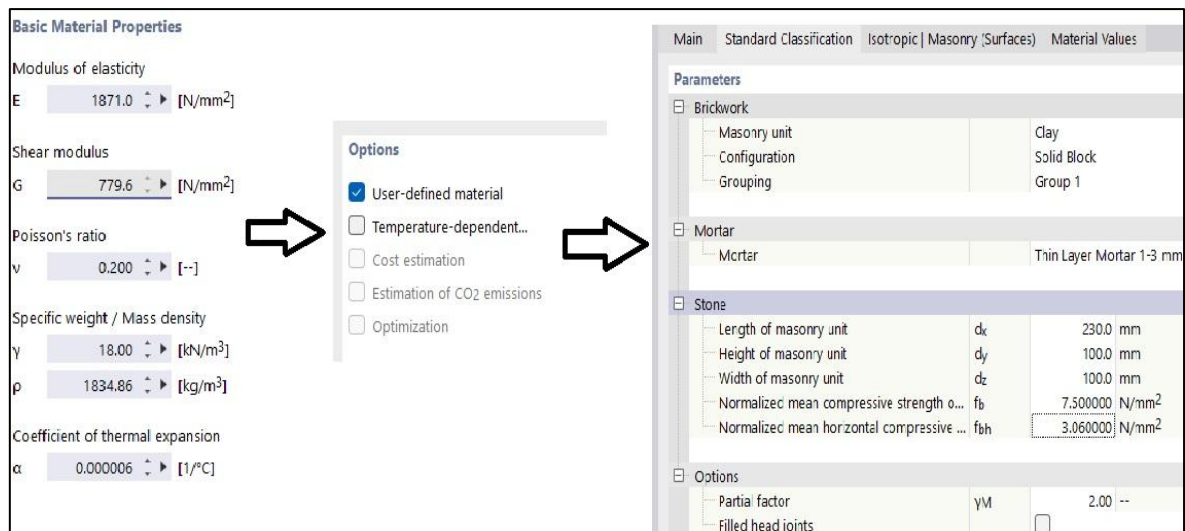
Figure 4. 6 Represents the material properties user defined

Below this image explains about different material properties of masonry: -

Type of Brick	Compressive strength (Mpa)
1st Class	10.297
2nd Class	6.865
3rd Class	3.4323

Cement:Sand	Compressive strength (Mpa)
01:03	10
01:04	7.5
01:05	5
01:06	3
01:08	0.7

7.9.2.1 The modulus of elasticity E_m (in MPa) of masonry infill wall shall be taken as:

$$E_m = 550 f_m$$

where f_m is the compressive strength of masonry prism (in MPa) obtained as per IS 1905 or given by expression:

$$f_m = 0.433 f_b^{0.64} f_{mo}^{0.36}$$

where

f_b = compressive strength of brick, in MPa; and
f_{mo} = compressive strength of mortar, in MPa.

1st class brick	Fm	Em
1	4.41187	2426.529
2	3.977817	2187.799
3	3.437573	1890.665
4	2.860134	1573.074
5	1.693784	931.5812

2nd class brick	Fm	Em
1	3.403595	1871.977
2	3.068739	1687.806
3	2.65196	1458.578
4	2.206488	1213.568
5	1.306692	718.6804

3rd class brick	Fm	Em
1	2.184049	1201.227
2	1.969176	1083.047
3	1.701734	935.9536
4	1.415879	778.7334
5	0.83849	461.1693

Figure 4.7 Represents the material properties as per IS codes

4.6 Boundary Conditions and Constraints

Support Conditions

In RFEM 6, fixed supports were assigned at the base of all masonry walls to represent the interface between the wall and foundation. These supports restrain all translational degrees

of freedom (UX, UY, UZ), simulating a rigid foundation system. Rotational degrees were assumed fully fixed for simplicity in linear and nonlinear seismic load applications.

Wall–Slab Connection

Although slabs in the model are reinforced concrete, the structural system remains URM because walls carry all vertical and lateral loads. There is no special diaphragm behavior modeled.

Instead:

The slabs are directly placed on walls, connected via shared nodes and boundary lines.

Load transfer is automatic through nodal continuity, which means no separate rigid link or interface element is modeled.

This approach ensures the vertical loads from slabs are fully transferred into the walls without additional modeling complexity, aligning with the simplified macro-modeling approach.

Openings and Load Paths

Openings such as doors and windows are modeled without restraints across them. This allows:

Accurate load redistribution around discontinuities,

Observation of localized cracking zones during pushover analysis
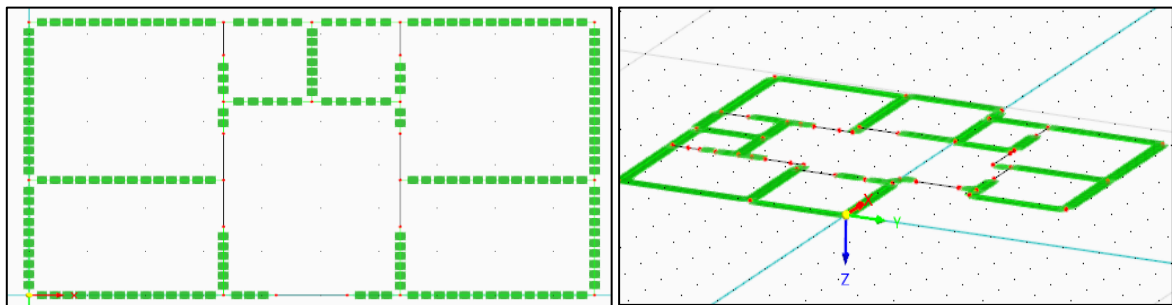
Figure 4.8 Represents the Rigid support used in the plans

4.7 Finite Element Meshing Strategy

The precision of finite element meshing is crucial in accurately simulating the seismic behavior of unreinforced masonry (URM) structures. In this study, RFEM 6 software, enhanced with the Masonry Design add-on, was utilized to develop a meshing approach that balances computational efficiency with analytical accuracy.

4.7.1 Selection of Mesh Elements

Masonry walls were represented using two-dimensional surface elements, effectively capturing both in-plane and out-of-plane behaviors essential for seismic analysis. This choice ensures that the structural response, including stress distributions and potential failure mechanisms, is accurately modeled.

4.7.2 Mesh Density and Refinement

An initial mesh size of 0.5 meters was adopted for the overall model, providing a balance between computational load and detail.
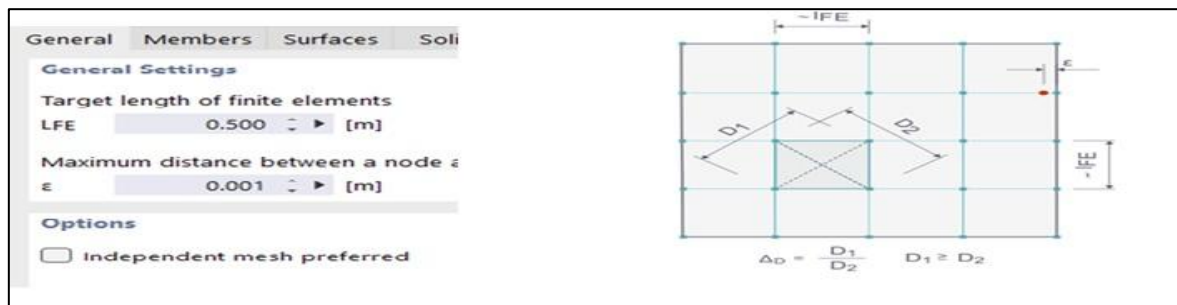
Figure 4.9 Mesh settings 0.5 m mesh used

To capture stress concentrations and potential crack initiation zones, mesh refinement was applied in critical areas such as:

Openings: Around doors and windows, where stress concentrations are anticipated.

Wall Intersections: At junctions between orthogonal walls, which are susceptible to complex stress interactions

Figure 4.10 Mesh used 0.3m

Support Regions: Near the base of walls and at points of load application, where reactions and stress intensities are significant.

Refined mesh sizes in these areas ranged from 0.2 to 0.3 meters, ensuring a more detailed analysis of stress variations and potential failure zones.

4.7.3 Ensuring Mesh Quality

Maintaining mesh quality is vital for the reliability of finite element analysis. In RFEM 6, mesh quality was assessed based on element aspect ratios, skewness, and connectivity.

Elements with poor aspect ratios or irregular shapes can lead to inaccurate stress predictions and convergence issues. Therefore, the mesh was iteratively refined, and quality checks were performed to maintain element integrity throughout the model.

4.7.4 Integration with Material Models

The meshing strategy was closely integrated with the nonlinear masonry plastic material models used for masonry in RFEM 6. Accurate meshing ensures that the material behavior, including cracking and crushing phenomena, is effectively captured. This integration is crucial for simulating the progressive failure mechanisms of URM structures under seismic loading.

4.7.5 Visualization and Validation

To validate the meshing strategy, visual inspections of the mesh were conducted within RFEM 6. Mesh overlays on the structural model allowed for the identification of irregularities and ensured that mesh refinement was appropriately applied in critical regions. Additionally, preliminary analyses were performed to assess the sensitivity of results to mesh density, confirming that the chosen meshing strategy provided a balance between accuracy and computational efficiency.

4.8 Load Combinations

In structural analysis, load combinations are essential to simulate realistic scenarios by combining various individual loads. In RFEM 6, these combinations help in assessing the structural response under different loading conditions.

The figure below illustrates the "Load Cases & Combinations" dialog box in RFEM 6, showcasing the configuration of load combinations. It highlights the use of the Combination Wizard, selection of analysis types (e.g., Geometrically Linear, Second-Order (P-Δ), Large Deformations), and the assignment of design situations.

4.11 Load cases interface and base settings

Table 1 Load cases and settings

Load Case	Name	To Solve	Analysis Type	Static Analysis Settings
LC1	Self-weight	+	Static Analysis	SA1 - Geometrically linear | Newton-Raphson
LC2	live load	+	Static Analysis	SA1 - Geometrically linear | Newton-Raphson
LC3	pushover force	+	Static Analysis	SA1 - Geometrically linear | Newton-Raphson
LC4	modal analysis	+	Modal Analysis	MOS1-fme: 90.00 % | Root of characteristic polynomial

4.8.1 Load Combinations for Modal Analysis

For modal analysis, it's crucial to define the mass distribution accurately, as it influences the natural frequencies and mode shapes of the structure. In your case:

- Dead Load (DL): Considered as self-weight.
- Live Load (LL): Included at 25% intensity.

Table 2 Load combination used for modal analysis

Load Combi.	Name	To Solve	Analysis Type	Static Analysis Settings	Design Situation
CO1	LC1 + 0.25 * LC2	+	Static Analysis	SA2 - Second-order (P-Δ) | Newton-Raphson | 100 | 1	DS1 - Limit State of Strength
CO2	LC1 + 0.25 * LC2 + LC3	+	Static Analysis	SA2 - Second-order (P-Δ) | Newton-Raphson | 100 | 1	DS1 - Limit State of Strength

This combination ensures that the mass participation from both permanent and transient loads is accounted for, which is vital for accurate dynamic analysis.

4.8.2 Load Combinations for Pushover Analysis

Pushover analysis involves applying lateral loads incrementally to assess the structure's capacity. Your approach includes:

- LC3 (EQX): Represents the lateral seismic load applied in the X-direction.
- DL + 0.25 LL: Serves as the constant vertical load during the pushover analysis.

This setup is appropriate, as it simulates the building's behavior under seismic loading while considering the gravity loads that would be present during such an event.

Table 3 Load combination used for pushover analysis

Load Combi.	Name	To Solve	Analysis Type	Static Analysis Settings
CO4	LC1+0.25*LC2	+	Pushover Analysis	SA2 - Second-order (P-Δ) | Newton-Raphson
CO5	LC3-PushoverX	+	Pushover Analysis	SA2 - Second-order (P-Δ) | Newton-Raphson

4.8.3 Analysis Settings

Modal Analysis: Utilized DL + 0.25 LL to define mass participation; computed sufficient modes to capture 90% mass in X and Y directions.

Pushover Analysis: Applied EQX as lateral load with constant DL + 0.25 LL; employed second-order (P-Δ) analysis with incremental loading until target displacement or collapse.

4.8.4 Verification and Validation

Consistency Check: Ensured uniform analysis settings across load combinations.

Preliminary Runs: Conducted initial simulations to verify model behavior and identify potential issues.

Result Assessment: Evaluated mode shapes and pushover curves to confirm realistic structural responses.

4.8.5 Modal Analysis Settings

Mass Import: Imported masses from a combination of Dead Load (DL) and 25% Live Load (LL) to accurately represent the structure's mass distribution for dynamic analysis.

Mode Calculation: Computed sufficient natural frequencies and mode shapes to capture the structure's dynamic behavior.

Mass Matrix: Utilized a consistent mass matrix to account for both translational and rotational degrees of freedom, enhancing the accuracy of modal results.
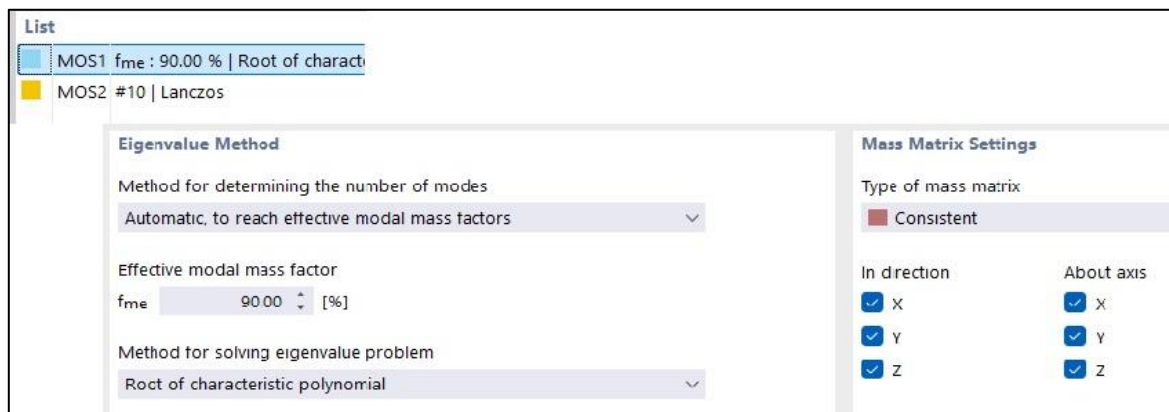
Figure 4.12 Modal analysis settings

4.8.6 Pushover Analysis Settings

Load Application: Applied incremental lateral loads in the X-direction (EQX) while maintaining a constant vertical load combination (DL + 0.25 LL) throughout the analysis.

Analysis Type: Employed second-order (P-Δ) nonlinear static analysis to capture the effects of geometric nonlinearity under increasing lateral loads.

Increment Control: Defined load increments and stopping criteria based on target displacement or structural instability indicators to ensure convergence and realistic simulation of structural behavior.
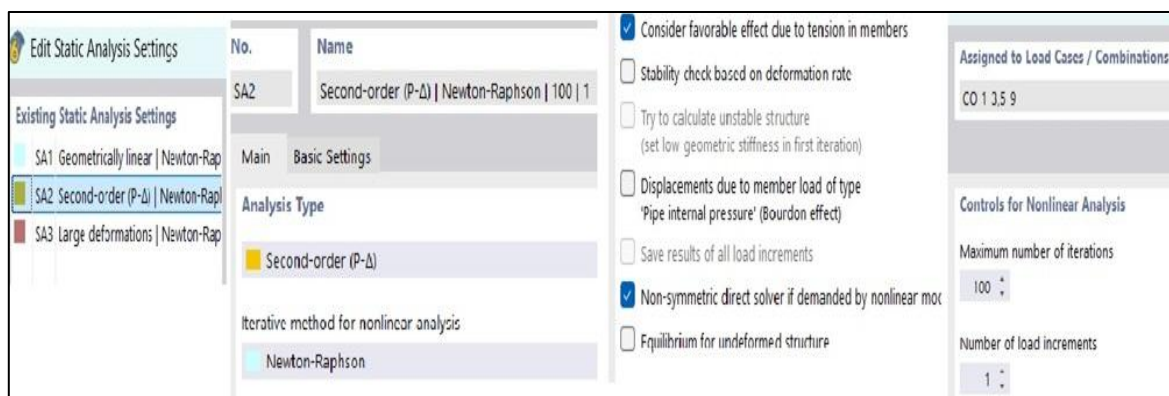
Figure 4.13 Pushover analysis settings

4.8.7 Response spectrum selection

The seismic response spectrum was defined based on IS 1893:2016 for Seismic Zone IV. The parameters used are as follows:

Table 4 Represents the response spectrum values used for analysis

SEISMIC ZONE	IV	
SEISMIC ZONE FACTOR Z	0.24	(Standards, 2016)
I IMPOTANCE FACTOR	1	
RESPONSE REDUCTION FACTOR	1.5	
Sa/g	2.5	
TIME PERIOD T	0.1936	

These values were input into the software to generate the design response spectrum used in the analysis. The spectrum governs the lateral seismic force distribution applied to the unreinforced masonry (URM) models
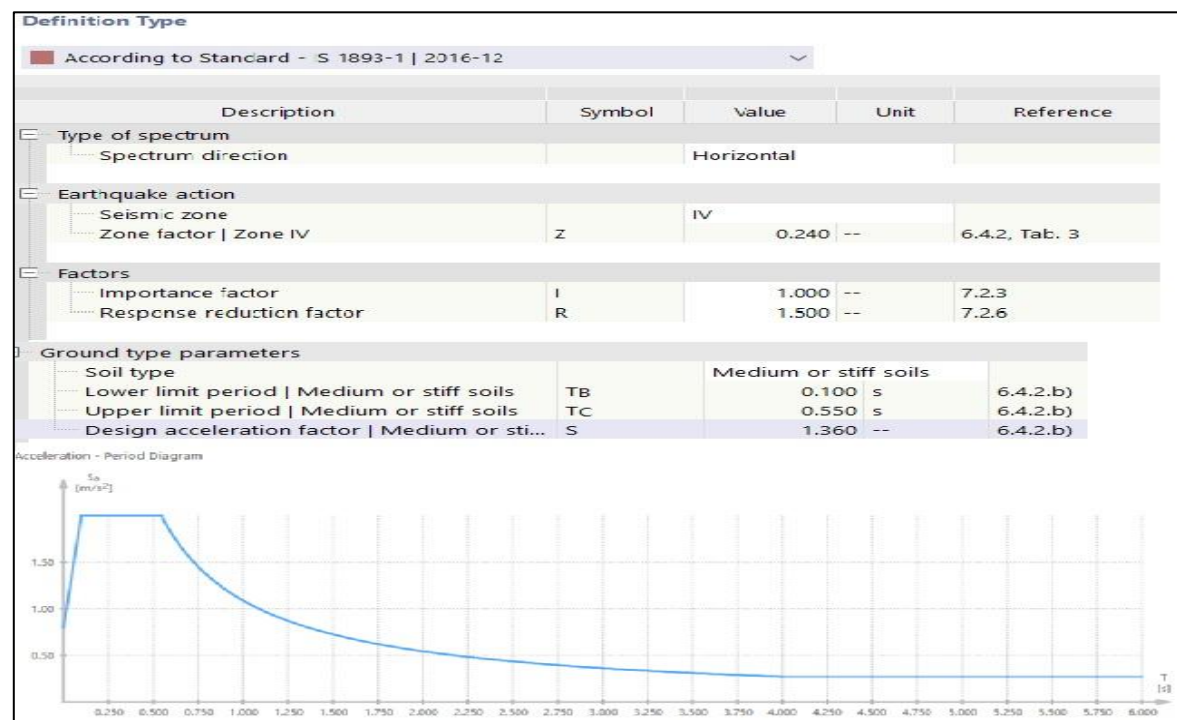
Figure 4.14 Represents the response spectrum used as per Indian standards

4.8.8 Modal Analysis Execution: Dynamic Behavior Evaluation

In this step, the modal analysis was performed to assess the dynamic characteristics of the URM building models. This analysis was essential to identify the natural frequencies and mode shapes that contribute to the building's seismic response. The results provide critical insights into the structure's vibrational behavior, helping to understand how it will perform under seismic loading.
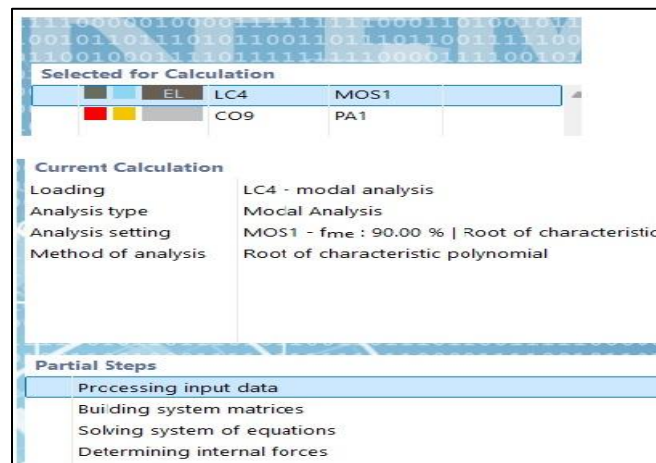
Figure 4.15 Calculation progress for modal analysis

4.8.9 Pushover Analysis Execution:

Following the modal analysis, the pushover analysis was executed to evaluate the nonlinear seismic response of the URM buildings. This method allows for a deeper understanding of the building's capacity to withstand lateral forces and identify its performance under extreme seismic conditions. It highlights key strength and stiffness characteristics, helping to evaluate the overall resilience of the structure.
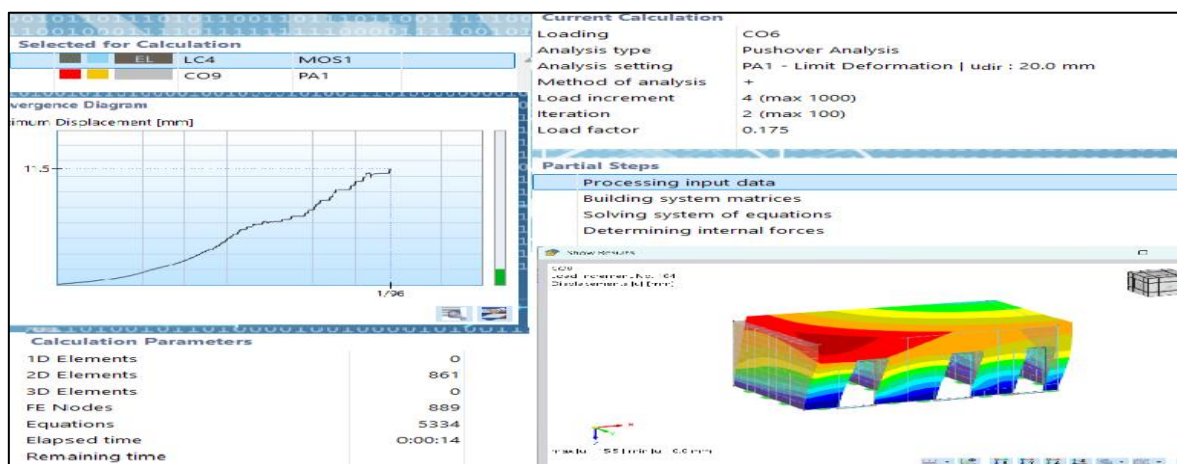
Figure 4.16 Calculation progress for pushover analysis

4.9 Summary:

In this chapter, the detailed modelling procedure was explained using **Model A** as an example. All steps, including geometry creation, meshing, load applications, and boundary conditions, were applied consistently to the other models (B, C, and D) following the same approach.

To provide clarity, images of the 3D models for all buildings have been included, illustrating the consistent application of the modelling steps. The results for each model will be discussed in the following chapter, where the **modal analysis** and **pushover analysis** outcomes will be presented and compared across all four-building configuration.

CHAPTER 5: RESULTS AND DISCUSSION OF MODAL AND PUSHOVER ANALYSIS

5.1 General Overview

This chapter presents the results of static and dynamic analyses conducted to evaluate the seismic response of Unreinforced Masonry (URM) buildings. The primary focus is on the modal analysis and pushover analysis, which provide valuable insights into the buildings' behaviour under seismic loading.

The seismic response of the URM buildings was evaluated using pushover analysis, a method that helps to assess the nonlinear behaviour of the structures under increasing lateral loads. The pushover curves for each model (A, B, C, and D) were analysed, focusing on parameters such as the effective modal mass, yield base shear, modal energy, and displacement at the performance point, among other key indicators of seismic behaviour. These analyses are crucial for understanding how each building responds to seismic forces and identifying potential failure mechanisms.

Table 5 Represents the model height and plan details

Model	Height (m)	Plan Symmetry	Wall Openings	Remarks
A	6.7	Asymmetric	Varying inner and outer openings	Irregular layout and variable wall lengths
B	3	Symmetric	Standard doors and windows	Uniform rooms, minor variation in layout
C	3	Symmetric	Similar to Model B	Slight room use difference, same wall layout

D	3.35	Symmetric	No external wall openings; 2 vents	Equal rooms, only internal doors, main entry

Additionally, modal analysis was performed to determine the dynamic characteristics of the buildings, including natural frequencies and mode shapes. This information is essential for understanding the structural response to seismic excitation and identifying vulnerabilities in the buildings' dynamic behaviour.

The models evaluated in this study differ in height, plan symmetry, and wall openings, which contribute to their unique seismic responses. The characteristics of each model are summarized in Table 6.1, providing an overview of the variations in layout and design features for Models A, B, C, and D. These variations are critical in understanding how each building may behave under seismic forces.

5.2 Modal Analysis Results

This section should summarize the results of the modal analysis, including the Effective Modal Mass, Modal Participation Factor, Displacement at Performance Point, and other key dynamic characteristics. You will compare the results across the four models to highlight how each design behaves dynamically

Table 6 Represents modal analysis results

Model	Mode No.	Eigenvalue (λ) [1/s²]	Angular Frequency (ω) [rad/s]	Frequency (f) [Hz]	Time Period (T) [s]	Direction of Vibration
A	1	3236.513	56.890	9.054	0.110	Translational
	2	3724.926	61.032	9.714	0.103	Translational
	3	6351.671	79.697	12.684	0.079	Rotational
B	1	6667.118	81.652	12.995	0.077	Translational
	2	6814.113	82.548	13.138	0.076	Translational
	3	10092.901	100.463	15.989	0.063	Translational
C	1	25782.331	160.569	25.555	0.039	Translational

	2	46431.019	215.479	34.294	0.029	Translational
	3	89522.752	299.204	47.620	0.021	Translational
D	1	13740.377	117.219	18.656	0.054	Translational mode
	2	20049.122	141.595	22.536	0.044	Torsional + Vertical Deformation Mode
	3	25292.284	159.035	25.311	0.040	Translational Mode along Y-axis

5.3 Pushover Analysis Results

The results from the pushover analysis provide insight into the effective modal mass and modal participation factors for each model, as detailed in Table 7. These parameters are essential for understanding the contribution of each building to the overall seismic response during a nonlinear dynamic event.

Modal Mass:

Model A demonstrates the highest effective modal mass, recorded at 161,841.2 kg. This suggests a substantial contribution of the building's mass to the seismic response, indicating that a larger portion of the structure is involved in the seismic motion.

Model B has a modal mass of 27,309.7 kg, which, while lower than Model A, still indicates significant involvement in the seismic response.

Model C exhibits the lowest modal mass at 9,705.7 kg, implying that a smaller proportion of the building mass participates in the seismic response. This result suggests that the structure's overall involvement during an earthquake is more localized compared to the other models.

Model D has a modal mass of 79,088.8 kg, suggesting a substantial contribution to the seismic response, although still lower than that of Model A.

Modal Participation Factor:

The modal participation factor reflects the extent to which each mode contributes to the seismic response. In this analysis:

Model A has a participation factor of $\Gamma = 1.228$, which, while relatively high, is slightly surpassed by Model B.

Model B shows a higher modal participation factor of $\Gamma = 1.370$, indicating a more distributed participation of the building's mass and stiffness in the seismic response. This

suggests that seismic forces are more uniformly spread throughout the structure in this model.

Model C shows a lower participation factor, consistent with its lower modal mass.

Model D exhibits a participation factor that falls between those of Model A and Model B. indicating a moderately distributed response across the structure.

Table 7 Represent the pushover results obtained from RFEM 6

Parameter	Model A	Model B	Model C	Model D
Effective Mass m* [kg]	1,61,909.30	27,309.70	9,705.70	79,088.80
Modal Participation φTφ [kg]	1,31,841.20	19,927.30	7,366.40	83,196.00
Modal Participation Factor Γ	1.228	1.37	1.318	0.951
Max Displacement dm* [mm]	27	7.9	15.7	10.9
Yield Base Shear Fy* [kN]	489.79	173.07	129.21	480.58
Energy Em* [J]	11,350.10	1,107.00	1,825.30	4,333.30
Yield Displacement dy* [mm]	7.6	3	3.1	3.8
Fundamental Period T* [s]	0.315	0.136	0.095	0.156
Spectral Acceleration Se(T*) [m/s2]	1.96	2	1.94	2.94
Target Displacement det* [mm]	4.9	0.9	0.4	1.8

Capacity Spectrum Period Tc [s]	0.55	0.55	0.55	0.55
Acceleration F$<y>$* / m* [m/s2]	3.03	6.34	13.31	6.08
Performance Point dt* [mm]	4.9	0.9	0.4	1.8
Ductility dm* / dt*	5.465	8.435	35.019	5.984
Collapse Displacement dt [mm]	6.1	1.3	0.6	1.7

These observations highlight the variability in seismic participation across the models. Model B stands out for its more distributed seismic response, while Model A exhibits significant participation, albeit less widespread. On the other hand, Model C shows a more localized response, with the lowest modal mass and participation factor, while Model D demonstrates a balanced seismic response.

In this section we have main focus on *Yield Base Shear (Fy), *Modal Energy (Em), *Effective Time Period (T), and other key parameters.

The pushover analysis was performed for each model to evaluate the structural performance under increasing lateral loads. Key results, such as the yield base shear and modal energy, are essential for understanding the nonlinear behavior of each structure. Model A exhibits the highest yield base shear (489.79 kN), reflecting its ability to resist lateral forces before yielding. In contrast, Model C has the lowest yield base shear (129.21 kN), indicating that it may be more vulnerable to lateral loads.

The Modal Energy shows how the structure's energy is distributed during seismic motion, with Model A having the highest value (11,350.1 J) and Model B the lowest (1,107 J). This indicates a higher level of energy absorption and dissipation capacity in Model A.

Additionally, the Effective Time Period (T*) for Model A (0.315 s) is significantly longer than that for Models B and C, which suggests a relatively flexible response in Model A. Models B and C have shorter periods, indicating stiffer responses to seismic loading

5.3.1 Graphical Comparison of Pushover Curves

To better understand the seismic performance of all four models under increasing lateral loads, the pushover curves are plotted below.

These curves represent the relationship between base shear and roof displacement and provide valuable insights into the structural behaviour of each model.

By examining these graphs, one can visually compare the stiffness, strength, and deformation capacity of the models.

- A steeper initial slope of the curve indicates higher lateral stiffness.
- The peak base shear reflects the strength of the structure.
- The ultimate displacement shows the structure's capacity to deform before failure.

Displacement at Performance Point The displacement at the performance point ($dm*$) represents the maximum lateral displacement that a structure experiences under equivalent seismic demand.

This value is critical for evaluating potential damage and structural integrity.

Model A exhibits the smallest displacement (7.5 mm), indicating a stiffer and more brittle response.

Model B shows the highest displacement (20.1 mm), suggesting greater flexibility and energy dissipation capacity.

Models C and D fall in the intermediate range with displacements of 15.7 mm and 10.9 mm, respectively, reflecting moderate ductility and structural response.

These observations highlight the varying seismic performance characteristics of each structural configuration.

Model A, while strong in initial resistance, may be more susceptible to brittle failure due to its limited deformation capacity.

Model B's higher displacement implies better ductility and a potential for sustained energy dissipation under seismic loads.

Models C and D demonstrate balanced behavior, combining moderate strength with sufficient deformation tolerance.

Understanding these variations is essential for selecting or improving design strategies in seismic-prone regions.

(c)

(d)
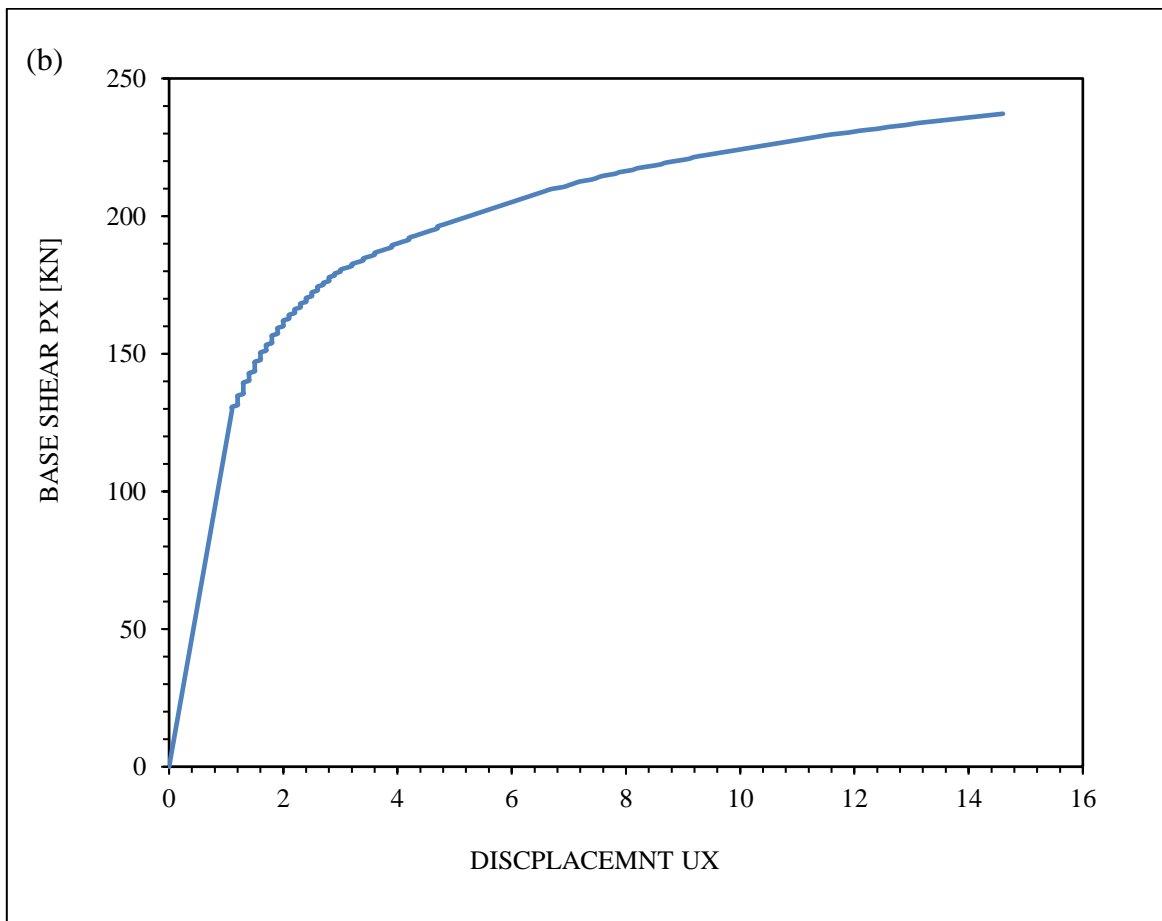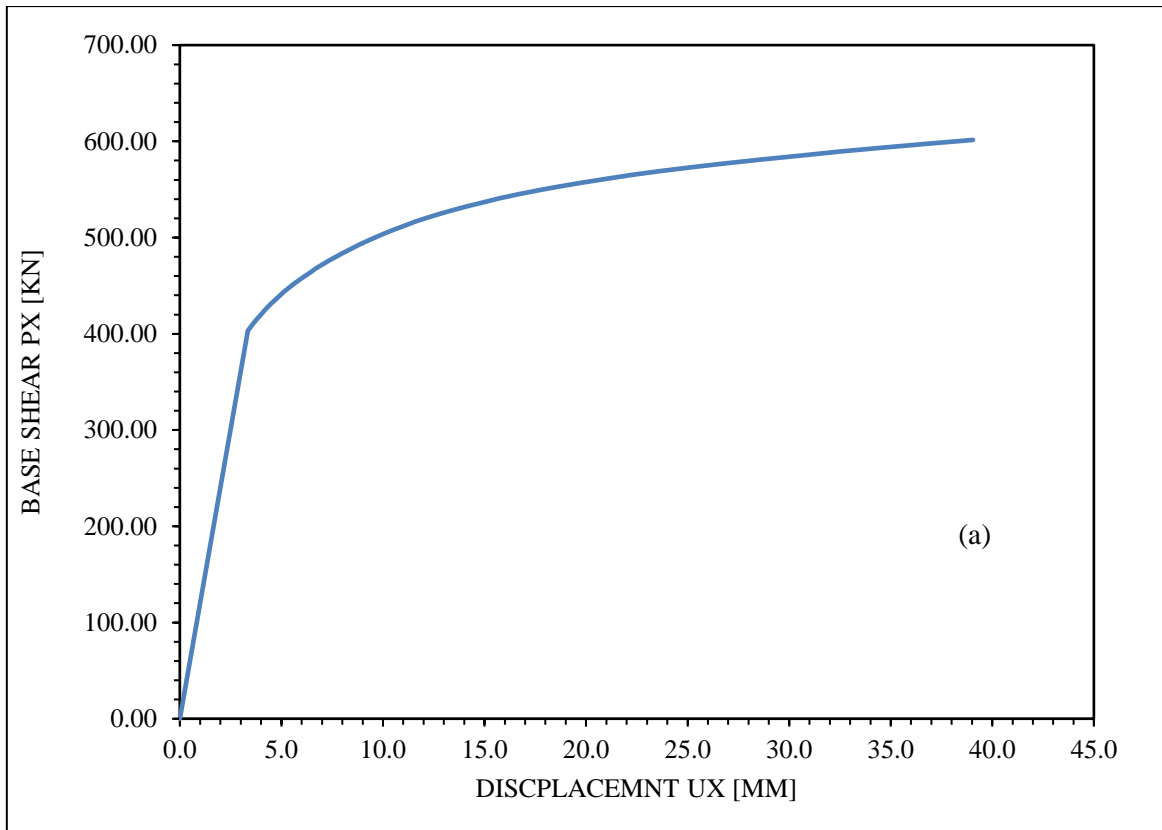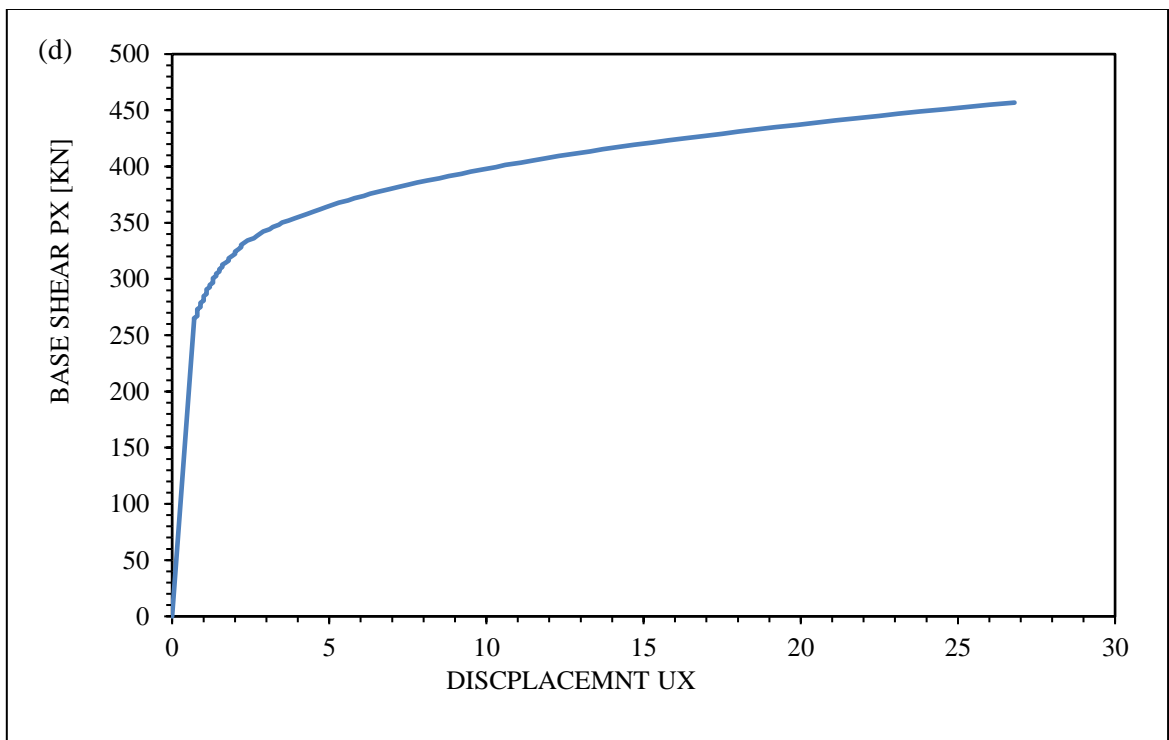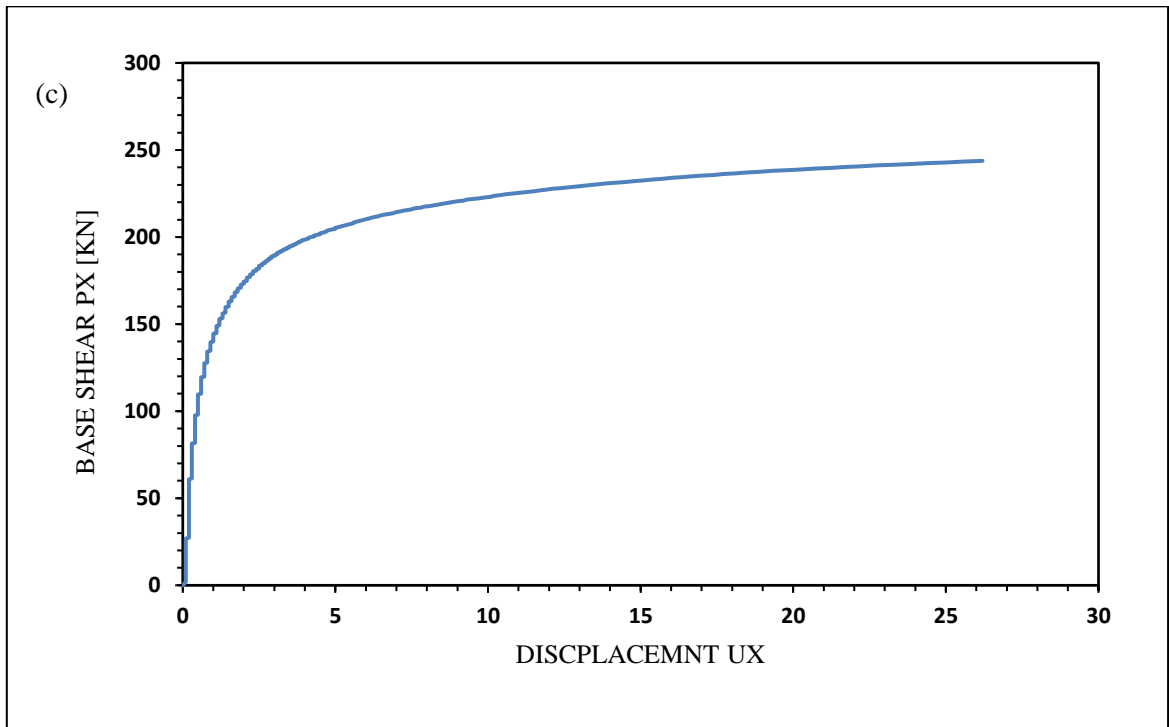
Figure 5. 1 Pushover analysis of selected Unreinforced masonry structures (a) Model A, (b) Model B (c) Model C (d) Model D

From the comparison:

Model A shows the highest base shear capacity and ductility.

Model B has moderate strength but a steep initial slope, showing higher stiffness.

Model C demonstrates the lowest capacity, indicating vulnerability.

Model D, despite high base shear, has relatively low displacement tolerance.

These observations correlate with the computed parameters in Table 6.3.1 and provide insight into the relative seismic performance of each structure.

5.3.2 Structural Behaviour Analysis

The structural behaviour of each model is inferred from both the numerical data and the pushover curves:

Model A: Displays strong lateral load resistance and moderate ductility, making it the most balanced in performance.

Model B: Despite being small in scale, it behaves stiffly but with limited energy dissipation.

Model C: Represents a two-story configuration, but lacks significant strength and stiffness.

Model D: Has good strength but limited ductility, with quick degradation beyond peak force.

The FEM analysis confirms that geometry, mass participation, and distribution of stiffness play a vital role in seismic performance. This comparative behaviour assists in vulnerability assessment and retrofits planning.

5.4 Performance Point Evaluation

The Performance Point Evaluation is a crucial step in assessing the seismic vulnerability of the four models using the Capacity Spectrum Method (N2 Method). This method provides a means to evaluate the seismic response by finding the intersection of the capacity and demand spectra. The performance point derived from this intersection signifies the maximum expected displacement and the corresponding base shear that each model will experience under a given seismic event.

5.4.1 Overview of the Capacity Spectrum Method

The Capacity Spectrum Method (N2 Method) is a widely recognized approach for evaluating the seismic response of structures. In this method, the capacity curve—obtained from the pushover analysis—is plotted against the demand spectrum, which represents the expected seismic forces. The intersection of these two curves identifies the performance point, a critical parameter that indicates the displacement at which the structure can no longer sustain

the applied seismic forces without significant damage. The target displacement at the performance point serves as a measure of the structure's lateral deformation during a seismic event.

5.4.2 Calculation of the Performance Point

The performance point for each model is determined by plotting the capacity curve and the demand spectrum on the same axes.

The displacement at the performance point, dm*, is then compared to the target displacement at the performance point, dt*.

The ratio of dm/dt** offers valuable insight into the relative flexibility or stiffness of the structure, with a higher ratio indicating greater flexibility and larger displacements under seismic loading.

Table 8 Shows the performance point and target displacement

Parameter	Model A	Model B	Model C	Model D
Displacement at Performance Point (dm*) [mm]	27	7.9	15.7	10.9
Target Displacement (dt*) [mm]	4.9	0.9	0.4	1.8
dm*/dt* Ratio [mm]	5.465	8.435	35.019	5.984

5.4.3 Evaluation of Performance Points

The results from the performance point evaluation reveal the following insights:

Model A: The displacement at the performance point (dm)* for Model A is 27.0 mm, which is relatively high compared to other models. With a dm/dt ratio of 5.465**, this indicates that Model A is relatively more flexible, experiencing higher displacements under seismic loading. This suggests that while the structure is capable of absorbing significant seismic energy, it may suffer higher deformations during a major seismic event.

Model B: In contrast, Model B exhibits a smaller displacement at the performance point (7.9 mm), with a dm/dt ratio of 8.435**. This higher ratio suggests that Model B is relatively

stiffer compared to Model A, and thus, it undergoes smaller displacements. Although this may be beneficial in terms of minimizing deformation, it also means the structure may be more susceptible to failure under extreme seismic conditions due to its limited flexibility.

Model C: Model C demonstrates a significant dm/dt ratio of 35.019**, which is the highest among the four models. Despite the relatively lower target displacement (0.4 mm), the displacement at the performance point reaches 15.7 mm. This large discrepancy highlights a significant vulnerability in Model C's design, suggesting that it may undergo catastrophic deformation during strong seismic events, potentially leading to structural collapse.

Model D: Model D shows a displacement at the performance point of 10.9 mm, with a dm/dt ratio of 5.984**. This places it between Models A and B in terms of flexibility. Although its displacement is smaller than that of Model A, it is larger than Model B, suggesting a balanced response in terms of seismic performance. This could indicate a reasonable compromise between flexibility and stiffness, resulting in moderate seismic deformations.

5.4.4 Implications of Performance Point Results

The performance point evaluation provides a comprehensive understanding of each model's seismic behavior.

Model A exhibits greater flexibility and displacement at the performance point, making it more capable of dissipating energy during seismic events but potentially leading to higher deformation and damage.

Model B, while stiffer, shows a higher dm/dt ratio, suggesting that it may experience limited deformation but could be more prone to brittle failure under severe seismic forces.

Model C displays significant vulnerability, with a high dm/dt ratio and large displacement at the performance point, indicating a greater risk of collapse under strong earthquakes.

Model D presents a balanced seismic response, making it more resilient to moderate seismic forces, though it may still experience some displacement during major events.

5.5 Comparative Discussion of Models

The comparative discussion aims to synthesize the results obtained from the pushover analysis and performance point evaluation for Models A, B, C, and D. By examining the key parameters such as displacement at the performance point, yield base shear, modal energy, and dm/dt ratios, we can gain insights into the relative seismic vulnerability of each model. This analysis will provide a deeper understanding of how each design responds to seismic forces and help identify which models perform better in terms of structural integrity and overall resilience.

5.5.1 Displacement and Flexibility

Displacement at the performance point serves as a key indicator of the flexibility of a structure. In this regard:

Model A shows the largest displacement (27.0 mm) at the performance point, indicating that it is the most flexible of the four models. While this flexibility allows the structure to dissipate seismic energy more effectively, it also leads to larger deformations. Such displacement could result in significant damage during a major seismic event, especially if the displacement exceeds the allowable limits for the building's use.

Model B, in contrast, experiences a smaller displacement at the performance point (7.9 mm), suggesting it is stiffer and undergoes less deformation. This lower displacement may imply better performance in terms of minimizing damage, but it also indicates that the structure might be more prone to brittle failure under extreme seismic forces. The higher dm/dt ratio (8.435) for Model B reflects this characteristic of stiffness combined with a relatively low displacement response.

Model C experiences a medium displacement (15.7 mm) but has the highest dm/dt ratio (35.019), indicating it undergoes a significant amount of deformation relative to its target displacement. This large discrepancy suggests that Model C might be highly vulnerable to collapse under strong seismic loading, making it less suitable for seismic design without further reinforcement or modifications.

Model D lies between Models A and B, with a displacement at the performance point of 10.9

mm and a dm/dt ratio of 5.984. This intermediate value indicates that Model D strikes a balance between flexibility and stiffness. It offers moderate seismic resistance, with lower displacement than Model A but higher than Model B, suggesting a reasonable compromise between energy dissipation and structural stability.

5.5.2 Yield Base Shear and Seismic Resistance

The Yield Base Shear is an important parameter that reflects the structural capacity to resist lateral forces before yielding occurs. The higher the yield base shear, the greater the structure's ability to withstand seismic forces.

Model A exhibits the highest yield base shear (489.79 kN), indicating a stronger capacity to resist seismic forces compared to the other models. This high base shear is consistent with the larger displacement observed in Model A, suggesting that while the structure can resist significant forces, it does so at the cost of undergoing substantial displacement.

Model B has the smallest yield base shear (173.07 kN), indicating that the structure is less capable of resisting lateral forces. This lower value is indicative of the structure's stiffer design, which leads to smaller displacements but also reduces its ability to absorb energy before yielding.

Model C shows a yield base shear of 129.21 kN, the second-lowest among the models. This, combined with the large displacement at the performance point, suggests that Model C may be particularly vulnerable to excessive seismic forces, making it less suitable for high seismic risk areas unless reinforced.

Model D has a yield base shear of 480.58 kN, which is close to that of Model A, suggesting that it possesses a similar level of capacity to resist lateral forces. The relatively moderate displacement at the performance point (10.9 mm) reflects a balance between structural stiffness and flexibility.

5.5.3 Modal Energy and Seismic Demand

Modal energy represents the energy absorbed by the structure during seismic loading, and it can be a useful indicator of how well a structure can dissipate seismic energy. Additionally, the Seismic Demand Se(T)* is a measure of the required seismic intensity.

Model A has the highest modal energy (11,350.1 J), indicating a high capacity to absorb and dissipate seismic energy. This energy dissipation capacity is vital in preventing catastrophic failure during seismic events, though the large displacement at the performance point suggests that it might experience significant damage despite its energy absorption capabilities.

Model B exhibits the lowest modal energy (1,107 J), suggesting that it absorbs relatively less seismic energy compared to the other models. However, this corresponds to the stiffer behavior of Model B, where less energy is required to induce deformation.

Model C also absorbs a moderate amount of energy (1,825.3 J), but the large displacement and high dm/dt ratio suggest that it may not adequately dissipate energy during severe seismic events, leading to potential structural failure.

Model D absorbs 4,333.3 J of energy, which is higher than Models B and C but lower than Model A. This places Model D in the middle ground, suggesting a balanced seismic energy dissipation capacity that complements its moderate displacement response.

5.5.4 Performance Summary and Recommendations

Model A exhibits a high yield base shear and modal energy absorption, but the significant displacement at the performance point indicates that it may be prone to considerable damage under high seismic forces. It could benefit from structural modifications to reduce its displacement or improve its stiffness without sacrificing its energy dissipation capacity.

Model B offers a stiffer design with smaller displacements but has a lower yield base shear, making it less capable of resisting large seismic forces. While this design minimizes deformation, it could benefit from improvements in its lateral force-resisting capacity to avoid brittle failure.

Model C demonstrates the greatest vulnerability, with a high dm/dt ratio and low yield base shear. This model is at risk of significant structural failure under seismic events, and considerable reinforcement or redesign is recommended to enhance its seismic resistance.

Model D provides a good compromise between flexibility and stiffness, with moderate displacements and a relatively high yield base shear. This model is likely to perform well in most seismic scenarios and is recommended for areas of moderate seismic risk.

5.6 Summary:

In this chapter, the seismic performance of four unreinforced masonry (URM) building models (A, B, C, and D) was evaluated through modal analysis, pushover analysis, and performance point evaluation using the Capacity Spectrum Method (N2 Method). The following key findings were derived from the analysis:

Modal Analysis: The modal analysis results showed significant variations in the natural frequencies, modal participation factors, and effective modal mass across the models. These differences highlighted the distinct dynamic behaviors of each building, with Model A being the most flexible and Model B exhibiting the highest modal participation factor, indicating its dominance in lateral vibration.

Pushover Analysis: The pushover analysis provided insight into the strength and deformation capacities of each model. Model A demonstrated the highest yield base shear, but its large displacement at the performance point indicated a more flexible and potentially vulnerable design. On the other hand, Model B showed a lower yield base shear and experienced less displacement, but its stiffer design makes it more prone to brittle failure under strong seismic loading.

Performance Point Evaluation: The performance point analysis, based on the capacity and demand spectra, revealed significant differences in the displacement at the performance point and the dm/dt ratios across the models. Model A and Model D exhibited higher flexibility, while Model B and Model C showed more stiffness but at the cost of reduced seismic energy absorption and potential failure under extreme conditions.

Comparative Discussion: A comparative discussion highlighted the relative strengths and vulnerabilities of each model. Model A and Model D demonstrated better overall seismic performance, with higher energy dissipation and moderate displacements. In contrast, Model B and Model C showed higher vulnerability to collapse, with Model C being the most prone to large deformations and failure.

Overall, the chapter provides a comprehensive understanding of the seismic behavior of the four URM models, emphasizing the need for structural improvements in certain designs, especially Model C, to ensure adequate seismic resile.

CHAPTER 6: SESIMIC VULNERABILITY ASSESSMENT

6.1 Introduction

The fragility curve serves as a valuable tool for predicting potential damage levels during an earthquake. Unreinforced masonry (URM) buildings are particularly vulnerable to earthquake-related damage due to their significant stiffness, substantial weight, and limited ductility. These structures are frequently found in rural areas of developing countries, such as India. In the event of a catastrophic failure, URM buildings can experience complete structural collapse, as evidenced by the Bhuj earthquake in 2001, illustrated in Fig. 7.1. Most research on performance-based seismic design relies on a deterministic approach. However, given the numerous uncertainties associated with material strength and earthquake forces, a probabilistic approach appears to be a more logical method for assessing a structure's performance. The HAZUS methodology is widely utilized to estimate potential losses in existing buildings caused by ground shaking during earthquakes, aiding in the quantification of seismic risk in specific regions or urban areas. Typically, a nonlinear pushover analysis of standard buildings is necessary to determine building capacity and establish fragility curves. This chapter outlines a procedure for developing the necessary fragility curves for various damage states, particularly focusing on the more severe damage scenarios, based on results from nonlinear pushover analyses. The fragility of a structure is defined as its vulnerability to damage from earthquake loading of a specified intensity. Fragility curves are considered one of the most effective tools for performance-based design, applicable to both new constructions and the evaluation of existing buildings in earthquake-prone regions worldwide for retrofitting purposes. Assessing the probability of different damage states is crucial for estimating earthquake-related losses. This probability is expressed in terms of the likelihood of reaching or surpassing a specific damage state based on ground motion severity, which may be represented by Peak Ground Acceleration (PGA) or spectral displacement. Various methods exist for developing fragility curves for different building types, utilizing either empirical data from past earthquakes or data derived from analytical simulations. In this study, the HAZUS method is employed to create the fragility curve for

a two-story clay URM wall. The ATC method defines ground motion in terms of PGA, while the HAZUS method considers spectral acceleration or displacement as the ground motion parameters. HAZUS damage functions for ground shaking consist of two components: one based on engineering parameters such as yield and ultimate strength derived from the pushover curve, known as the capacity curve, and the other being fragility curves that describe the probability of damage across four distinct damage states. (Washington)

Figure 6.1 Bhuj earthquake damage to URM, 2001

The HAZUS Earthquake Loss Estimate Methodology for Buildings

The methodology for estimating earthquake losses in buildings using HAZUS is visually represented in Figure 7.1. This methodology consists of several modules, which will be briefly introduced and discussed in the subsequent sections. The different damage grades, referred to as Gr1, Gr2, Gr3, and Gr4, are explained in the following sections. The damage states, as defined by Barbat et al. (2006), are based on the yield and ultimate spectral displacements of a building and are utilized in this study. This approach ensures a comprehensive understanding of the potential impacts of earthquakes on structures.
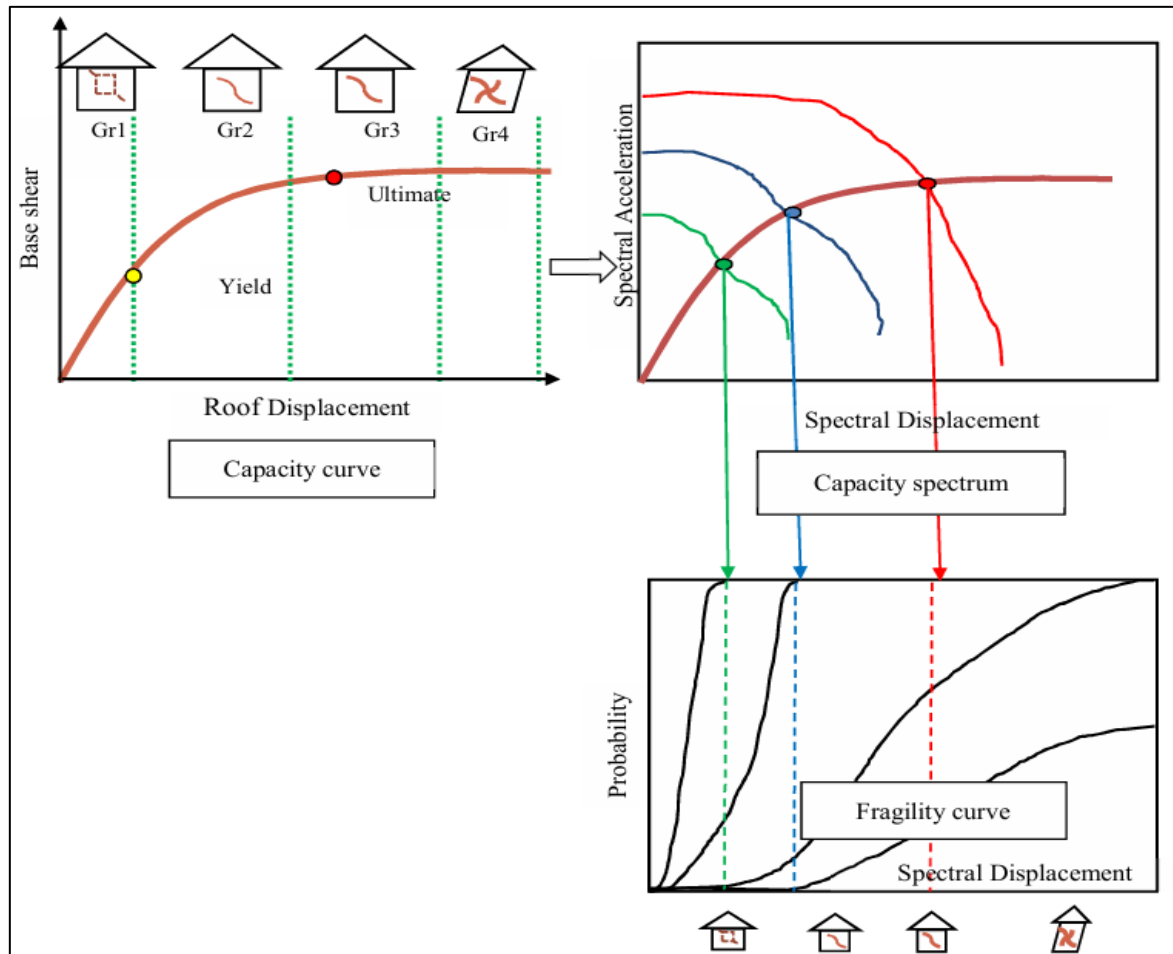
Figure 6.2 HAZUS earthquake loss estimate methodology for buildings (HAZUS 2003)

6.2.1 Development of Fragility Curves for URM

Fragility curves are characterized as log-normal distributions that depict the probability of achieving or exceeding a certain threshold of structural or non-structural damage. In this context, the median estimate of spectral response, which pertains to spectral displacement in this research, is established. This relationship is mathematically expressed as shown in Equation 6.1.

$$p\left[\frac{d_s}{s_d}\right] = \phi\left[\frac{1}{\beta_{ds}}\ln\left(\frac{s_d}{\bar{s}_{d,ds}}\right)\right]$$

where:

$\emptyset$ is known as a normal cumulative distribution function,

β_{d_s} is the variability parameter obtained from standard deviation of natural logarithm of the spectral displacement for damage state ds,

$\bar{s}\,d,ds$ is the median spectral displacement at which building reaches the threshold of damage state ds.

6.2.2 Variability Parameter (β_{ds})

$$\beta_{ds} = \left\{ \left(CONV\left[\beta_{c,}\beta_{D,}\bar{s}_{d,ds} \right] \right)^2 + \left(\beta_{M(ds)} \right)^2 \right\}^{\frac{1}{2}}$$

where:

β_c is the lognormal standard deviation parameter showing variability in capacity properties of the building,

β_d is the variability in the demand spectrum due to spatial variability of the ground motion,

β_M is the uncertainty in the estimation of the0damage state threshold.

 The overall variability associated with structural damage can be viewed as the combination of the three types of damage variability outlined in the preceding equation, utilizing a complex convolution method. HAZUS MR1 has supplied pre-calculated values of βds to eliminate the need for intricate numerical computations. The variability figures are presented in Table 6.1 based on the assumptions made in the research. Nevertheless, HAZUS has established a consistent moderate variability for the damage state threshold, β-, m-, ds... at 0.4, while the variability for the capacity curve is defined as β-s at 0.3. The variability resulting from post-yield degradation for Gr3 damage states, accounting for minor degradation, is 0.9, whereas for Gr4 damage states, considering significant degradation, it is 0.5. Consequently, the total variability, β-M, dS... for Gr2 damage state is 0.95, for Gr3 it is 1.05, and for Gr4, it is also taken as 1.05. (Washington)

6.2.3 Damage States

Damage states give an idea of building physical conditions, which are related to various loss parameters, like an economic loss, functional loss etc. The damage states defined by Barbat et al. (2006) based on yield and ultimate0spectral0displacements of a0building are used in the present work. This is shown in Table 6.2 given below Damage states provide insights into the physical condition of buildings, which are associated with different loss parameters, such as economic and functional losses. The damage states established by Barbat et al. (2006), which are based on yield and ultimate spectral displacements of a building, are utilized in this study. This information is presented in Table 6.2 below.

Damage state definition (Barbat, 2006)

Table 9 Damage state definition (Barbat, 2006)

Damage grade	Damage state	Spectral displacement
Gr1	Slight damage	$0.7S^{dy}$
Gr2	Moderate damage	S^{dy}
Gr3	Extensive damage	$S^{dy} + 0.25(S^{du} - S^{dy})$
Gr4	Complete damage	S^{du}

6.3 HAZUS-Based Fragility Assessment of URM Models

This section presents the HAZUS-generated fragility curves and corresponding damage state distributions for each of the four unreinforced masonry (URM) models analysed. The fragility curves indicate the probability of exceeding different damage states under increasing seismic intensity, while the pie charts visually represent the proportion of buildings expected to fall within each damage category (Slight, Moderate, Extensive, Complete) at the performance point.

Table 10 Classification of Damage States Based on Mean Damage Index (HAZUS Framework)

Most probable damage state	Mean damage index range
No damage	0 to 0.5
Slight damage	0.5 to 1.5
Moderate damage	1.5 to 2.5
Severe damage	2.5 to 3.5
Complete damage /collapse	3.5 to 4.0

6.3.1 Model A – Fragility and Damage Distribution Analysis

Figure 6.3 presents the fragility curves generated for Model A using the HAZUS methodology. Under Design Basis Earthquake (DBE) conditions, the model shows an overwhelmingly high probability (99.7%) of experiencing no damage, with negligible probabilities of slight (0.32%) and moderate damage (0.15%). Under Maximum Considered Earthquake (MCE), the structure becomes moderately vulnerable, with a 72% probability of slight damage and 38% for moderate damage. Severe and complete damage states remain low at 6.9% and 0.33%, respectively.

- **Mean Damage Index under DBE:** 0.2539
- **Mean Damage Index under MCE:** 1.241

It is important to note that these results show **unrealistically low damage probabilities under DBE**, suggesting that the structure is not failing even under increased lateral demands. This may be attributed to limitations or inaccuracies in modelling parameters, idealized material assumptions, or the absence of critical failure modes such as out-of-plane mechanisms. Since unreinforced masonry is inherently brittle and prone to sudden failure, the performance seen here does not fully align with expected real-world behaviour, and thus, further refinement or validation is recommended

Table 11 Performance Point (P.P) Coordinates for DBE and MCE

P.P LINE FOR DBE	
0	2.55
1	2.55
P.P LINE FOR MCE	
0	9.36
1	9.36

Table 12 Probability of Exceedance for Each Damage State under DBE and MCE

DAMAGE	DBE	MCE
slight	0.0032	0.72
moderate	0.0015	0.38
severe	0	0.069
complete	0	0.0033

Table 13 Damage Metrics and Mean Damage Indices for DBE and MCE Scenarios

AVERAGE OF MEAN DAMAGE INDEX		PROBABILITY OF OCCURANCE		DSM	MCE
NO DAMAGE	0.25	0.9968	0.28	0.2492	0.07
SLIGHT	1	0.0017	0.34	0.0017	0.34
MODERATE	2	0.0015	0.311	0.003	0.622
SEVERE	3	0	0.0657	0	0.1971
COMPLETE	3.75	0	0.0033	0	0.012375
		1	1	**0.2539**	**1.241**

6.3 Fragility Curves (Sd vs Probability of Exceedance) for Model A
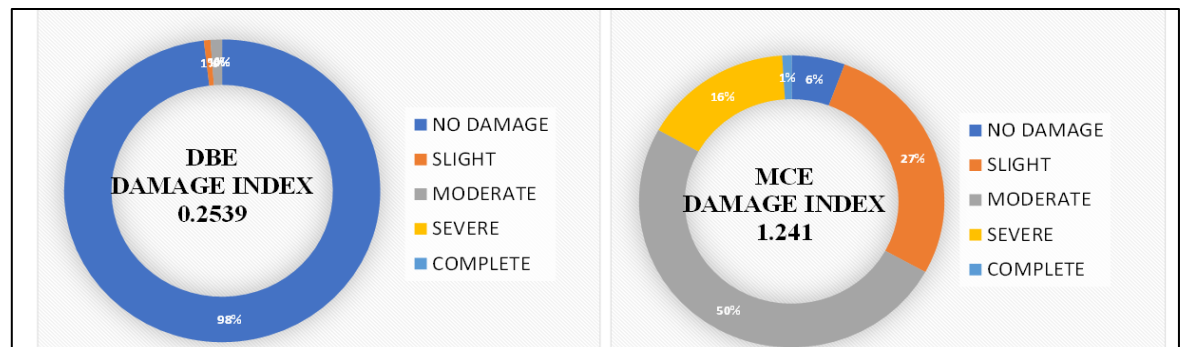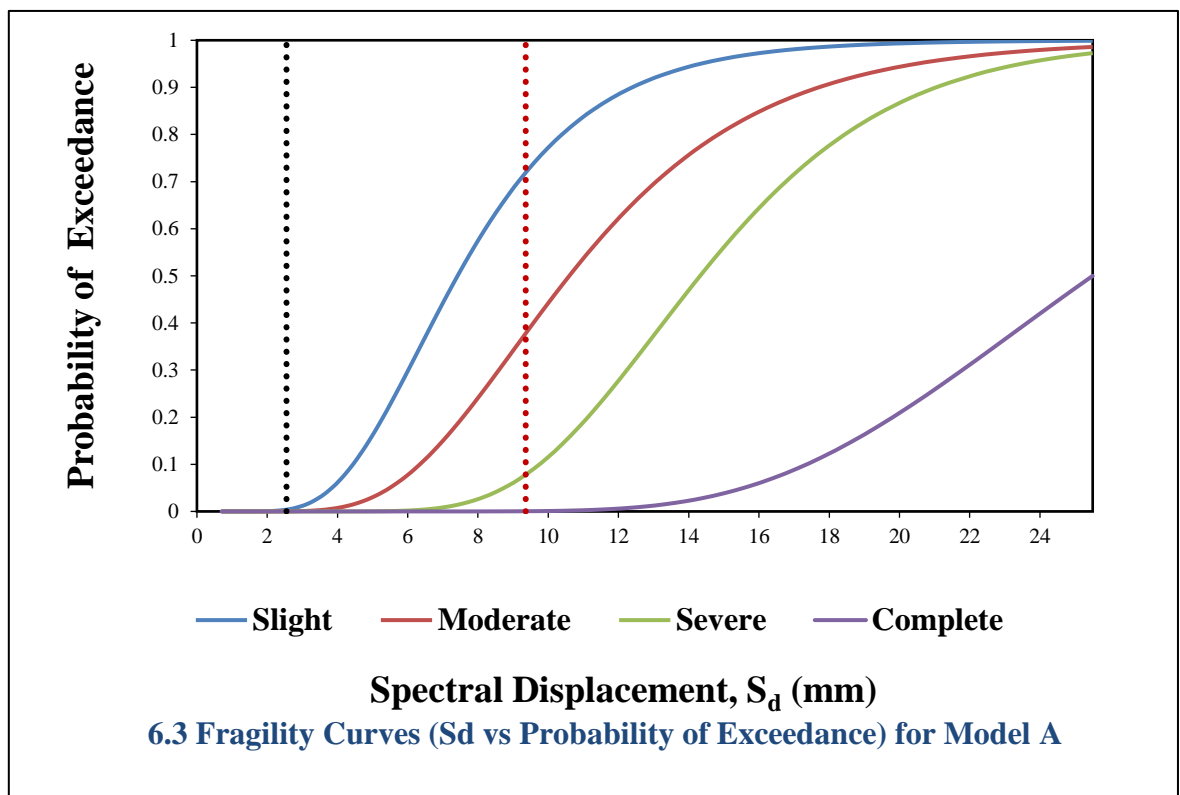
Figure 6.4 Pie chart representing the damage of building

6.3.2 Model B – Fragility and Damage Distribution Analysis

The fragility curves for Model D, shown in Figure 6.5, highlight a relatively improved performance under DBE, with no damage probability at 54.9%, and slight and moderate damage at 29.6% and 13.7%, respectively. However, under MCE, the building shows significant vulnerability: complete damage reaches 23.8%, while moderate and severe damage probabilities climb to 91% and 67.2%, respectively.

- **Mean Damage Index under DBE:** 0.7493
- **Mean Damage Index under MCE:** 3.054

As presented in Figure 6.6 (a & b), the pie charts visually confirm the high vulnerability under MCE conditions. A vast majority of the structure transitions to severe or complete failure modes under extreme shaking, indicating structural inadequacy at high displacement levels.

Table 14 Performance Point (P.P) Coordinates for DBE and MCE

P.P LINE FOR DBE	
0	2
1	2
P.P LINE FOR MCE	
0	6.34
1	6.34

Table 15 Probability of Exceedance for Each Damage State under DBE and MCE

DAMAGE	DBE	MCE
slight	0.451	0.996
moderate	0.155	0.968
severe	0.006	0.91
complete	0	0.238

Table 16 Seismic Damage Metrics and Mean Damage Indices for DBE and MCE Scenarios

AVERAGE OF MEAN DAMAGE INDEX		PROBABILITY OF OCCURANCE		DSM	MCE
NO DAMAGE	0.25	0.549	0.004	0.13725	0.001
SLIGHT	1	0.296	0.028	0.296	0.028
MODERATE	2	0.149	0.058	0.298	0.116
SEVERE	3	0.006	0.672	0.018	2.016
COMPLETE	3.75	0	0.238	0	0.8925
		1	1	**0.7493**	**3.054**

Figure 6.5 Fragility Curves (Sd vs Probability of Exceedance) for Model B
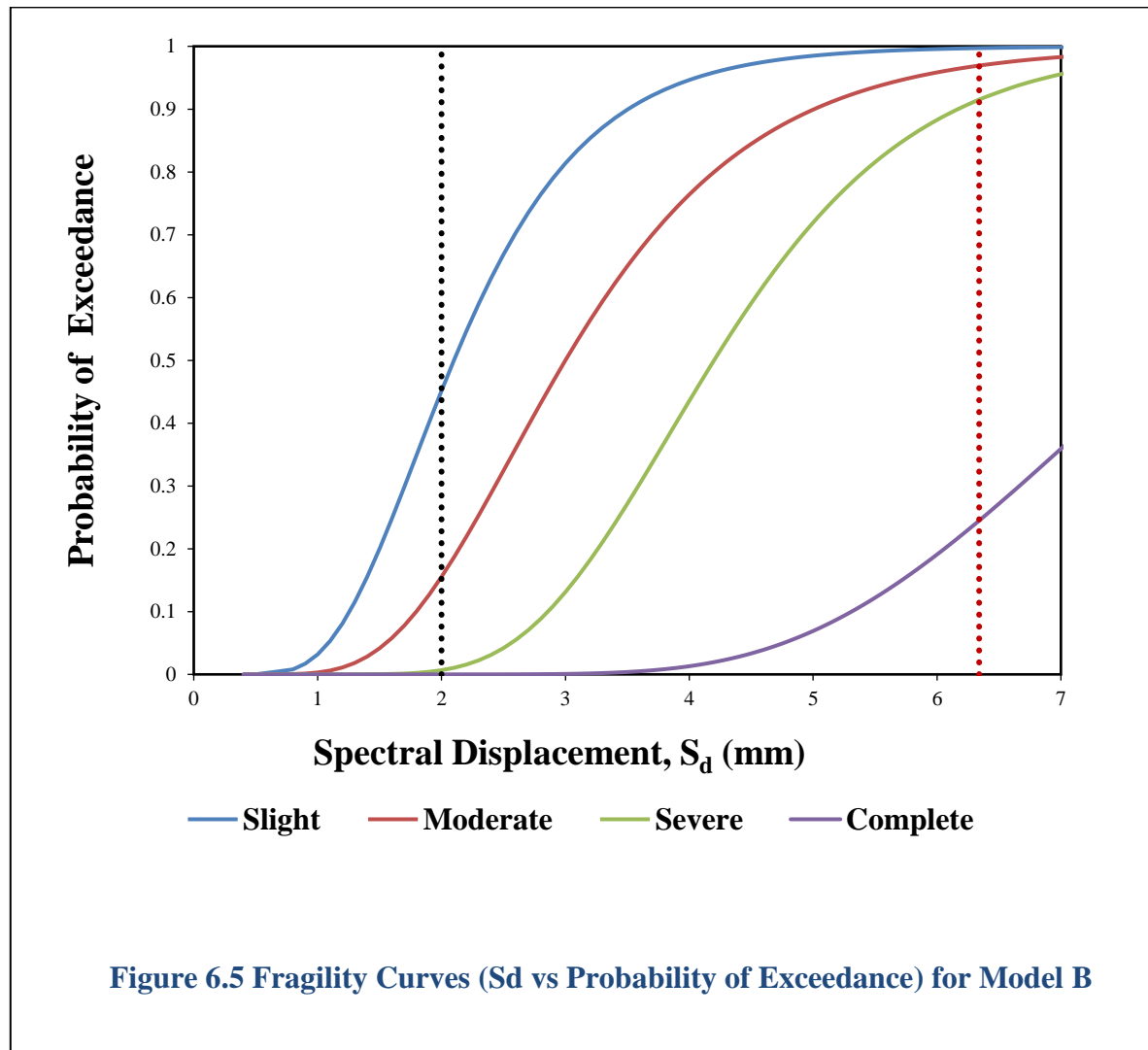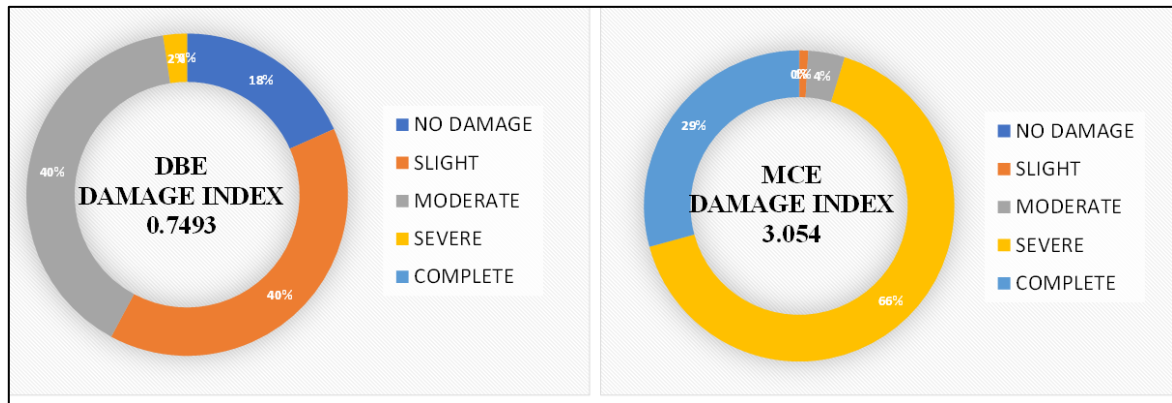
Figure 6.6 Pie chart representing the damage of building

6.3.3 Model C – Fragility and Damage Distribution Analysis

The fragility curves for Model C, shown in Figure 6.7, indicate moderate performance under DBE conditions. The probability of no damage is approximately 63.1%, while slight and moderate damage occur at 25.85% and 11.05%, respectively. No probabilities are recorded for severe or complete damage under DBE, reflecting a reasonably good response at design-level excitation. Under MCE, the performance degrades significantly. The structure experiences complete damage with a probability of 27.3%, and severe damage reaches 72%. Additionally, moderate damage is observed with a 22.1% probability.

- **Mean Damage Index under DBE:** 0.6373
- **Mean Damage Index under MCE:** 3.196

As presented in Figure 6.8 (a & b), the pie charts clearly reflect this contrast in performance. While DBE results show a predominance of no to slight damage, the MCE scenario is marked by a shift towards severe and complete failure modes, confirming Model C's high vulnerability under extreme seismic demands.

Table 17 Performance Point (P.P) Coordinates for DBE and MCE

| P.P LINE FOR DBE	
0	1.92
1	1.92
P.P LINE FOR MCE	
0	13.31
1	13.31

Table 18 Probability of Exceedance for Each Damage State under DBE and MCE

DAMAGE	DBE	MCE
slight	0.369	0.999
moderate	0.1105	0.999
severe	0	0.993
complete	0	0.273

Table 19 Seismic Damage Metrics and Mean Damage Indices for DBE and MCE Scenarios

AVERAGE OF MEAN DAMAGE INDEX		PROBABILITY OF OCCURANCE		DSM	MCE
NO DAMAGE	0.25	0.631	0.001	0.15775	0.00025
SLIGHT	1	0.2585	0	0.2585	0
MODERATE	2	0.1105	0.006	0.221	0.012
SEVERE	3	0	0.72	0	2.16
COMPLETE	3.75	0	0.273	0	1.02375
		1	1	**0.6373**	**3.196**
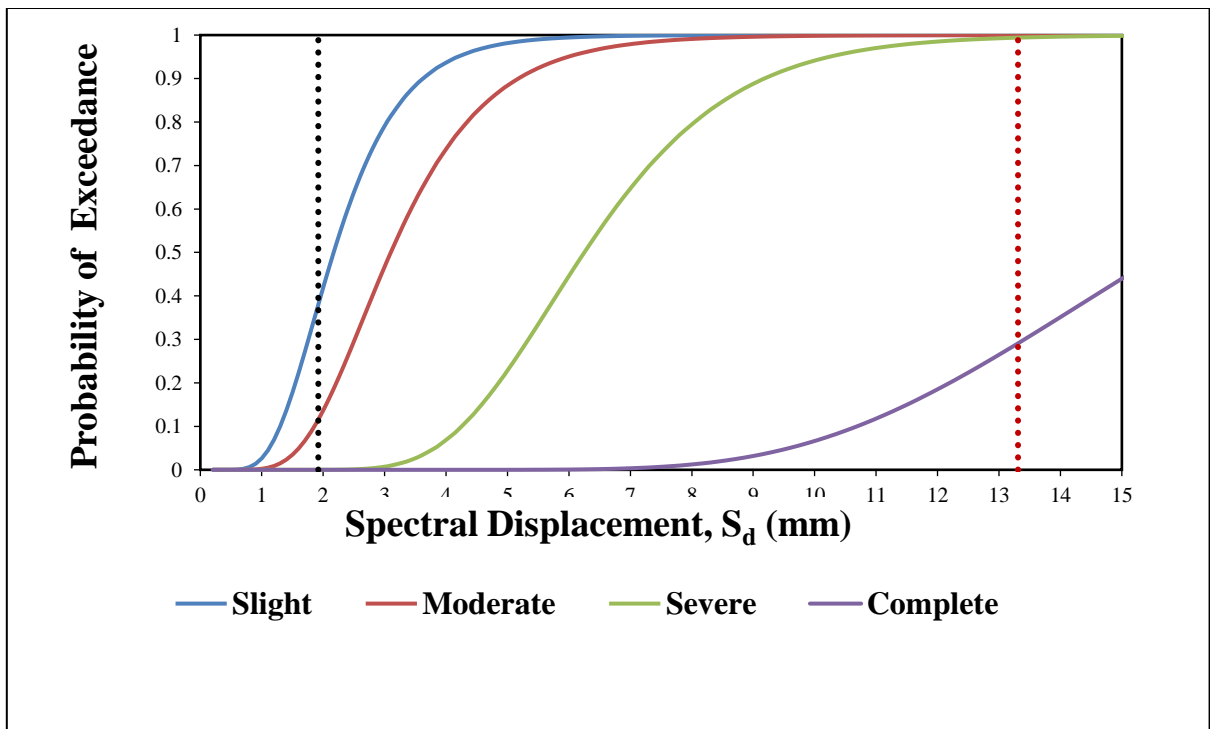
Figure 6.7 Fragility Curves (Sd vs Probability of Exceedance) for Model C
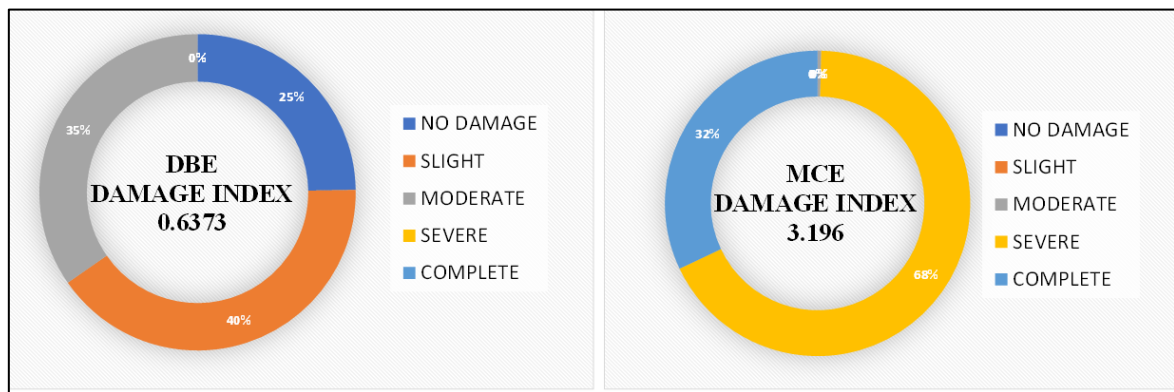
Figure 6.8 Pie chart representing the damage of building

6.3.4 Model D – Fragility and Damage Distribution Analysis

Figure 6.9 shows the fragility curves generated using the HAZUS methodology for Model D. The curves indicate that under Design Basis Earthquake (DBE), the probability of slight damage is approximately 58.7%, while moderate and severe damage probabilities are 25.3% and 1.4%, respectively. For Maximum Considered Earthquake (MCE), the building is highly vulnerable, with a 99.1% chance of slight damage and 72.9% probability of severe damage.

Mean Damage Index under DBE: 0.9573

Mean Damage Index under MCE: 2.687

Figure 6.10 (a & b) displays the pie charts representing the damage state distributions. Under DBE, the model experiences a balanced distribution across no, slight, and moderate damage states. Under MCE, damage becomes significantly severe, with a considerable share falling under the severe and complete damage states.

**Table 20 Performance Point (P.P) Coordinates for DBE and MCE**

P.P LINE FOR DBE	
0	2.94
1	2.94
P.P LINE FOR MCE	
0	6.08
1	6.08

Table 21 Probability of Exceedance for Each Damage State under DBE and MCE

DAMAGE	DBE	MCE
slight	0.587	0.991
moderate	0.253	0.923
severe	0.014	0.729
complete	0	0.0553

Table 22 Seismic Damage Metrics and Mean Damage Indices for DBE and MCE Scenarios

AVERAGE OF MEAN DAMAGE INDEX		PROBABILITY OF OCCURANCE		DSM	MCE
NO DAMAGE	0.25	0.413	0.009	0.10325	0.00225
SLIGHT	1	0.334	0.068	0.334	0.068
MODERATE	2	0.239	0.194	0.478	0.388
SEVERE	3	0.014	0.6737	0.042	2.0211
COMPLETE	3.75	0	0.0553	0	0.207375
		1	**1**	**0.9573**	**2.687**
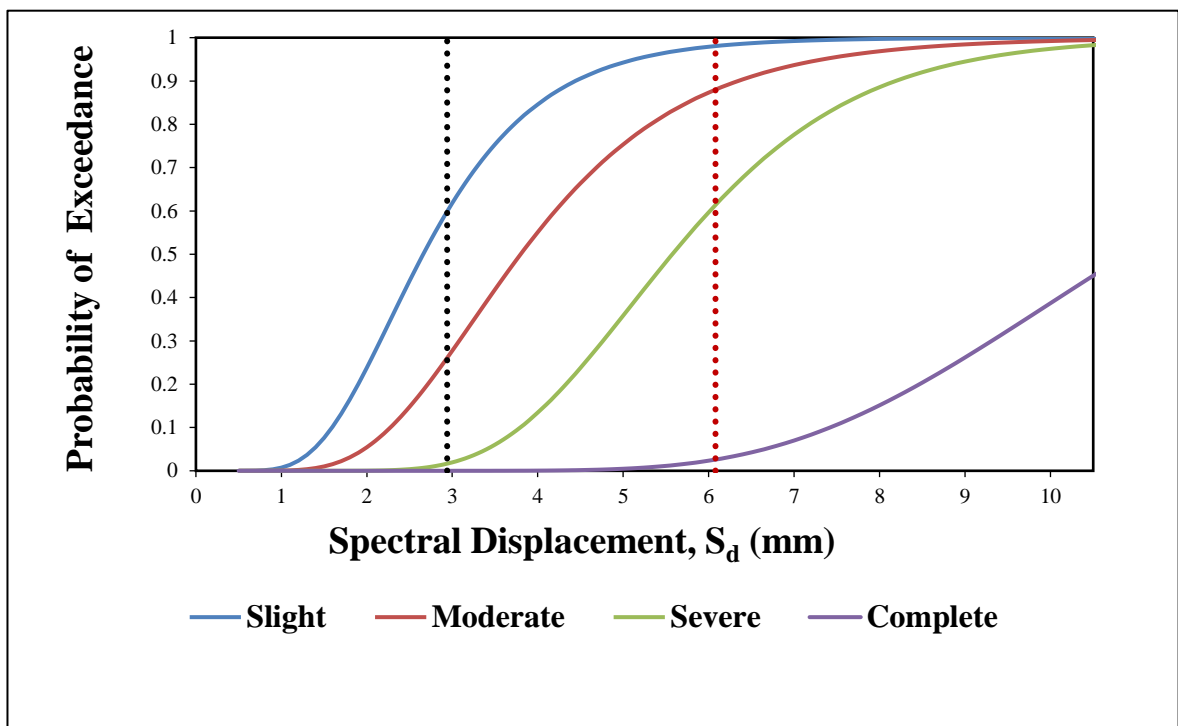
Figure 6.9 Fragility Curves (Sd vs Probability of Exceedance) for Model D
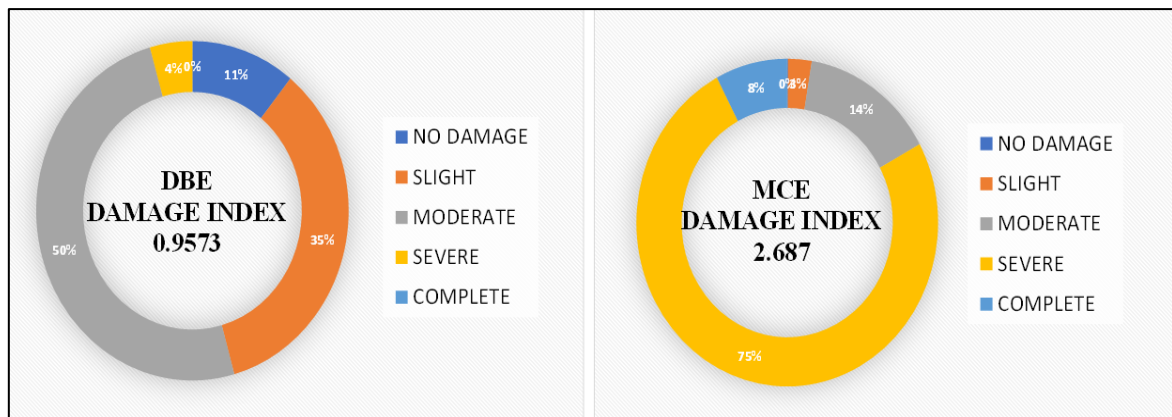
Figure 6.10 Pie chart representing the damage of building

6.4 Summary

This chapter presents a comprehensive seismic vulnerability assessment of unreinforced masonry (URM) buildings using fragility curves developed in accordance with the HAZUS methodology. The objective is to quantify potential damage probabilities under varying seismic intensities—primarily the Design Basis Earthquake (DBE) and Maximum Considered Earthquake (MCE)—and evaluate the seismic performance of structures based on their likelihood of exceeding specific damage states.

HAZUS fragility functions are probabilistic tools that relate structural damage states (slight, moderate, severe, and complete) to spectral displacement. These functions are developed by fitting lognormal cumulative distribution curves that reflect the probability of damage exceedance as seismic demand increases. Damage state thresholds are defined based on spectral displacement values, and performance point data from pushover analysis are used to extract relevant probabilities.

In addition to fragility curves, pie charts are employed to depict the distribution of buildings across different damage states, providing a visual interpretation of vulnerability under DBE and MCE scenarios. The results demonstrate a marked increase in damage severity from DBE to MCE, highlighting the heightened risk associated with more extreme ground motions. The Mean Damage Index (MDI), calculated as a weighted average based on the probability of occurrence and damage level severity, serves as a key metric in quantifying structural degradation.

Overall, the HAZUS-based approach proves effective in identifying the relative vulnerability

of URM, enabling prioritization for retrofitting or detailed risk mitigation strategies. The outcomes underline the importance of seismic intensity in shaping structural performance and reinforce the need for targeted resilience planning in seismically active regions.

CHAPTER 7 CONCLUSION

7.1 Summary of the Present Study

This study presents a comprehensive seismic vulnerability assessment of unreinforced masonry (URM) buildings using real-life building plans from the Jammu and Kashmir region. The assessment is performed using the Capacity Spectrum Method, based on nonlinear static analysis conducted in RFEM 6. The models reflect actual construction geometries and layouts observed in the field. The research workflow includes modal analysis, pushover analysis, performance point evaluation using the N2 method, and fragility curve development in accordance with HAZUS guidelines.

7.2 Major Conclusions

- URM buildings based on actual residential layouts demonstrate high seismic vulnerability, especially under Maximum Considered Earthquake (MCE) scenarios.
- Modal analysis shows that irregular mass distribution and asymmetry increase dynamic response and susceptibility to seismic forces.
- Pushover curves reveal early stiffness degradation and brittle failure patterns typical of URM construction without seismic detailing.
- The Capacity Spectrum Method provides a reliable estimation of realistic performance points, critical for seismic safety assessment.
- HAZUS fragility curves and pie charts offer valuable insights into probabilistic damage distribution, highlighting the need for policy-level mitigation strategies in similar urban settings.

7.3 Practical Implications

- The use of real-life structural plans increases the practical relevance of this study, enabling local authorities and engineers to understand actual seismic performance of existing masonry stock.

- The methodology developed can be applied directly to assess and rank buildings for seismic retrofitting in vulnerable regions.
- The results can inform disaster preparedness, urban planning, and risk-sensitive land use policies.

7.4 Limitations of the Study

- The models do not account for construction quality variation, ageing, or material degradation common in existing URM buildings.
- The analysis is limited to in-plane behaviour, neglecting possible out-of-plane wall failures, which are common in URM structures during earthquakes.
- Dynamic time-history analysis and field validation were not included due to resource constraints.

7.5 Scope for Future Work

- Extend the analysis to include more diverse building typologies and regional variations in URM construction practices.
- Incorporate nonlinear time-history analysis with a suite of real ground motion records for more accurate seismic response.
- Investigate combined in-plane and out-of-plane behaviour and soil-structure interaction effects.
- Develop a seismic vulnerability map for URM buildings using GIS tools, informed by the fragility data generated.
- Collaborate with local authorities for field validation, community-level assessments, and the creation of a regional URM fragility database.

References

1. Abide Aşıkoğlua, G. V. (2020). Pushover analysis of unreinforced irregular masonry buildings: Lesson from different modelling approaches Journal. *Engineering Structures (Elsevier)*, 218, 110830.

2. Cosgun, T. U. (2022). Seismic vulnerability assessment of a masonry structure and an FRP-strengthening proposal. *Case Studies in Construction Materials*, 17, e01680.

3. Council, A. T. (1996). ATC 40. *Seismic evaluation and retrofit of concrete buildings*, 1, 346.

4. Endo, Y. P. (2017). Review of different pushover analysis methods applied to masonry buildings and comparison with nonlinear dynamic analysis. *Journal of Earthquake Engineering*, 21(8), 1234-1255.

5. Giordano, A. G. (2008). Pushover analysis of plan irregular masonry buildings. *In Proceedings of the 14th World Conference on Earthquake Engineering* (pp. 12-17). Beijing China: World Conference on Earthquake Engineering.

6. Gonçalves, M. P. (2024). Seismic Assessment of Existing Masonry Buildings Using Damage Mechanics. *Buildings*, (2075-5309), 14(8).

7. Khattak, N. D. (2024). Seismic vulnerability assessment of pre-1945 unreinforced masonry buildings located in Queensland, Australia, using an index-based approach. *In Structures Elsevier*, Vol.67,p.106900.

8. Lipika Halder, S. P. (2021). "Seismic Vulnerability assessment of low-rise unreinforced Masonry Buildings in Northeast India Considering Variability of Material Properties". *Asian Journal of Civil Engineering (Springer)*.

9. Penelis, G. G. (2006). An efficient approach for pushover analysis of unreinforced masonry (URM) structures. *Journal of Earthquake Engineering*, 10(03), 359-379.

10. Shabani, A. K. (2021). State of the art of simplified analytical methods for seismic vulnerability assessment of unreinforced masonry buildings. Engineering Structures. *Enngieering Structures*.

11. Singh, Y. L. (2013). An analytical study on the seismic vulnerability of masonry buildings in India. *Journal of Earthquake Engineering*, 399-422.

12. Standards, B. o. (2016). *Bureau of Indian Standards.* Retrieved from Bureau of

Indian Standards: https://www.bis.gov.in/

13. Wani, F. M. (2023). Finite element analysis of unreinforced masonry walls with different bond patterns. *Sustainable Engineering and Innovation*, 5(1), 58-72.

14. ATC 40 (1996), Seismic Evaluation and Retrofit of Concrete Buildings: Vol. 1, Applied Technology Council, USA

15. Eurocode 8 (2004), Design of Structures for Earthquake Resistance, Part-1: General Rules, Seismic Actions and Rules for Buildings, European Committee for Standardization (CEN), Brussels.

16. FEMA 356 (2000), Pre standard and Commentary for the Seismic Rehabilitation of Buildings, American Society of Civil Engineers, USA.

17. FEMA 440 (2005), Improvement of nonlinear static seismic analysis procedures, Applied Technology Council (ATC) Washington, D.C. 10.

18. FEMA 273 (1997), NEHRP Guidelines for the seismic rehabilitation of buildings. Federal Emergency Management Agency, Applied Technology Council, Washington D.C., USA. 11.

19. FEMA 274 (1997), NEHRP Commentary on the Guidelines for the Seismic Rehabilitation of Buildings. Federal Emergency Management Agency, Applied Technology Council, Washington D.C., USA.

20. IS 1893. (2016). Indian Standard Criteria for Earthquake Resistant Design of Structures, Bureau of Indian Standards, New Delhi.

21. IS: 1905-1987. (1989). Code of practice for structural use of unreinforced masonry. *Bureau of Indian Standards*.

22. IS 2212. (1991). Brick Work - Code of Practice, Bureau of Indian Standards, New Delhi. 16.

23. IS 3828 (1976), "Improving Earthquake Resistance of Low Strength Masonry Buildings – Guidelines", Bureau of Indian Standards, New Delhi. 17.

24. IS 456 (2000). Indian Standard for Plain and Reinforced Concrete - Code of Practice, Bureau of Indian Standards, New Delhi.

25. SP 20 (S&T). (1991). Code of Practice for Structural use of Un-reinforced Masonry, Bureau of Indian Standards, New Delhi.

26. Dlubal RFEM 6 gratis de Dlubal, Z. (2022). RFEM 6. *Enfoque*, *2593*, 001781.

APPENDICES

APPENDIX-A

Abbreviations and notations

Symbol / Notation	Description
T	Natural Period of Structure (sec)
f	Natural Frequency (Hz)
ω	Angular Frequency (rad/s)
λ	Eigenvalue (1/s²)
m*	Effective Modal Mass (kg)
$\varphi^T\varphi$	Modal Participation Factor
Γ	Modal Participation Coefficient
d_m*	Displacement at Effective Mass Point (mm)
F_γ*	Yield Base Shear (kN)
E_m*	Strain Energy at Effective Mass Point (Joules)
d_γ*	Yield Displacement at Effective Mass (mm)
T*	Equivalent SDOF Period (sec)
Se(T*)	Spectral Acceleration at T* (m/s²)
d_{et}*	Displacement at Equivalent Time (mm)
d_t	Target Displacement (mm)
Tc	Characteristic Period (sec)
F_γ*/m*	Acceleration Capacity (m/s²)
d_m*/d_t*	Displacement Ductility Ratio
S_a	Spectral Acceleration
Sd	Spectral Displacement
ADRS	Acceleration-Displacement Response Spectrum

N2 Method	Nonlinear Static Analysis Method (Eurocode 8 based)
FEMA	Federal Emergency Management Agency (USA)
HAZUS	Hazard U.S. Earthquake Loss Estimation Method
URM	Unreinforced Masonry
RFEM	Finite Element Software used for Structural Modelling and Analysis
DBE	Design Basis Earthquake
MCE	Maximum Considered Earthquake
DSM	Damage State Median
DCE	Design Check Earthquake
SME	Serviceability Minor Earthquake

APPENDIX-B

Review Card: - INTERNAL REVIEW-I (3730002)

Gujarat Technological University
Master of Engineering (Dissertation Review Card)
Effective from Academic year 2024-25.

Date: 21 / 9 / 2024

Semester:	3	Subject Name & Code:	Internal Review -1 3730002	IR-1

Student's Enrollment:	2 3 1 3 7 0 7 2 0 8 2 0	
Name of Student:	VISHWASH RUKWAL	
Student's Mail ID: -	Official vishwash @ outlook.com	
Students Contact No.	9103435001	Branch Code: 020
Theme of Dissertation:	FEM	Branch Name: STRUCTURAL Engg.

Title of Dissertation: Seismic Vulnerability assessment of UN-Reinforced Masonry Buildings Using Capacity-Spectrum based Method

Sr. No.	Comments given by Internal review panel. (Please write specific comments)	Modification done based on Comments
1.	Collect more literature on various Mathematical modelling of masonry structures.	Done
2.	design URM building as per IS, Euro, ACI using Dubel Software	
3.		

Guide's Signature

Note:
Above suggestions/modifications/comments must be fulfil/accommodate by the student in DP 1

Approved ✓
Not Approved

Please tick on any one.
If approved, then put marks ≥ 50 %.

Internal Review Panel

Particulars		
Name:	Dr. J.A. Amin	Parvidul Seth
Institute code & Name:	GTU - SET - 137	GTU-SET - 137
Mobile No.:	9925543275	9374710086
Signature:		n seth

Internal Guide's Details

Particulars		
Name:	Dr. Kaushik Gondaliya	
Institute code & Name:	GTU - SET - 137	
Mobile No.:	7016143139	
Signature:	k.m.gondaliya.	

APPENDIX-C

Review Card: - Dissertation Phase-I (3730003)

Gujarat Technological University
Master of Engineering (Dissertation Review Card)

Date: 07 / 12 / 2024

Hall No: _____

Effective from Academic year 2024-25.

Semester:	3	Subject Name & Code:	Dissertation Phase 1 - 3730003	DP-1

Student's Enrollment: 2 3 1 3 7 0 7 2 0 0 2 0

Name of Student: Vishwash Rukwal

Student's Mail ID: - Official.vishwash @ outlook.com

Students Contact No. 9103435001

Branch Code: 020

Branch Name: Structural Engg.

Theme of Dissertation: FEM

Title of Dissertation: Seismic Vulnerability assessment of UN Reinforced Masonry Buildings using Capacity Spectrum based Method

OBSERVATIONS

1. Appropriateness of title with proposal. (Yes/ No) _Yes_
2. Whether the selected theme is appropriate according to the title? (Yes / No) _Yes_
3. Justify rational of proposed research. (Yes/ No) _Yes_
4. Clarity of objectives. (Yes/ No) _Yes_

Sr. No.	Comments given by External Examiners (DP-I) (Please write specific comments)	Modification done based on Comments
—	Work on Real' life problem of building.	
—	Check the feasibility of Software for further Analysis.	? Done
—	Try to Include more buildings with irregularities to increase comparche parameters	
—	Also justify the method considered in the present work	

*If modification in title is suggested by experts, then student is required to submit duly signed title change form after taking mail approval from experts.

Guide's Signature: k.n.gondaliya

Note:
Above suggestions/modifications/comments must be fulfil/accommodate by the student in IR-2

Approved ✓
Not Approved

Please tick on any one.
If approved, then put marks ≥ 50 %.

Details of External Examiner

Particulars	Expert 1	Expert 2
Name:	Dr. C. S. Sanghvi	Dr. C. N. Patel
Institute code & Name:	028 LDCE	019 - VGEC, A'bad
Mobile No.: (optional)	94283 50436	99252 23693
Email Id:	cssanghvi @ ldce.ac.in	cnpatel.693@ gmail.com
Signature:		

APPENDIX-D

Review Card: - Internal Review-II (3740001)

Gujarat Technological University — Master of Engineering (Dissertation Review Card)	Date: 16 / 04 / 2025

Effective from Academic year 2024-25.

Semester:	4	Subject Name & Code:	Internal Review -2 – 3740001	IR-2

Student's Enrollment:	2 3 1 3 7 0 7 2 0 0 2 0		
Name of Student:	VISHWASH RUKWAL		
Student's Mail ID: -	Official vishwash @ outlook.com	Branch Code	020
Students Contact No.	9103435001	Branch Name	Structural Engg.
Theme of Dissertation:	FEM		
Title of Dissertation:	Seismic Vulnerability assessment of Un-Reinforced Masonry Buildings using Capacity Spectrum Based Method.		

Sr. No.	Comments given by Internal Examiners (IR-2) (Please write specific comments) i) The appropriateness of the major highlights of work done; State here itself if work can be approved with some additional changes. ii) Main reasons for approving the work. iii) Main reasons if work is not approved.	Modification done based on Comments
—	Consider the material Property of masnory as per the regional or IS code and perform the Pushover analysis.	Done
		K.M.gondaliya Guide's Signature

Note:
Above suggestions/modifications/comments must be fulfil/accommodate by the student in DP-2

Approved ✓
Not Approved

Please tick on any one.
If approved, then put marks ≥ 50 %.

Details of Internal Examiner

Particulars	Internal Review Panel	Internal Review Panel
Name:	Dr. J.A. Amin	Prof. Mridul Seth
Institute code & Name:	GTU - SET - 137	GTU - SET - 137
Mobile No.:	9925543275	9374710086
Email Id:	Prof.jignesh @ gtu.edu.in	
Signature:	Jm	m.seth

APPENDIX-E

Plagiarism Report

Vishwash Rukwal

Seismic Vulnerability Assessment of Un-reinforced Masonry Buildings Using Capacity Spectrum-based Method

📄 Quick Submit
🖥 Quick Submit
🎓 Gujarat Technological University

Document Details

Submission ID
trn:oid:::1:3224735031

Submission Date
Apr 22, 2025, 4:39 PM GMT+5:30

Download Date
Apr 22, 2025, 4:40 PM GMT+5:30

File Name
231370720020_vishwash_ME-SE_-_THE_Boss.pdf

File Size
3.7 MB

65 Pages

13,880 Words

80,749 Characters

🔷 turnitin   Page 2 of 76 - Integrity Overview   Submission ID trn:oid:::1:3224735031

22% Overall Similarity

The combined total of all matches, including overlapping sources, for each database.

Match Groups

🔴 189 Not Cited or Quoted 18%
Matches with neither in-text citation nor quotation marks

🟠 21 Missing Quotations 3%
Matches that are still very similar to source material

🟡 4 Missing Citation 1%
Matches that have quotation marks, but no in-text citation

🔵 3 Cited and Quoted 0%
Matches with in-text citation present, but no quotation marks

Top Sources

16% 🌐 Internet sources
15% 📖 Publications
9%   👤 Submitted works (Student Papers)

Integrity Flags

1 Integrity Flag for Review

🚩 Hidden Text
117 suspect characters on 1 page
Text is altered to blend into the white background of the document.

Our system's algorithms look deeply at a document for any inconsistencies that would set it apart from a normal submission. If we notice something strange, we flag it for you to review.

A Flag is not necessarily an indicator of a problem. However, we'd recommend you focus your attention there for further review.

Signature and Name of Student

Vishwash Rukwal

231370720020

Signature and Name of Guide

Dr. Kaushik Gondaliya

Assistant Professor, GTU-SET

APPENDIX-F

Problem Validation

F.1.1 Collection of data from the referred paper

A. Giordano, M. Guadagno and G. Faella, ''PUSHOVER ANALYSIS OF PLAN IRREGULAR MASONRY BUILDING The 14th World Conference on Earthquake Engineering" (Giordano, 2008). [Microsoft Word - 14-0257.doc](#)

Paper Type: The 14th World Conference on Earthquake Engineering

Authors: - M. Guadagnuolo, G. Faella, A. Giordano

Source: - M. Guadagnuolo, G. Faella, A. Giordano "PUSHOVER ANALYSIS OF PLAN IRREGULAR MASONRY BUILDINGS, The 14th World Conference on Earthquake Engineering October 12-17, 2008, Beijing, China

Methodology Overview

Finite Element Method (FEM) approach using Dlubal RFEM-6

Key steps taken:

Modeling of masonry structure.

Applying dead load, live load, and other forces.

Performing Modal Analysis

F.1.1.1 Collection of data from the referred paper

Table 23 Data of Problem Validation

Geometry	
Length in X-Direction	24m
Length in Y direction	11.10m
Height of building	7.0m
Height of each floor	3.5m
Dead load	5 KN/m2
Live load	2 KN/m2
Wall type	Unreinforced masonry wall

Floor and slabs	0.15m for ground and 0.2m for top
Number of stories	2
Type of buildings	Symmetric, Asymmetric
Youngs's Modulus Em	1500 MPa
Tangent Modulus	200MPa
Compression Strength f_{mc}	2MPa
Tensile strength f_{mt}	0.1MPa
Volumetric mass	17kN/m3
Live load	2 KN/m2
Slabs and floor	Assumed C25/30 as per Eurocode 2 (EN 1992-1-1: Unreinforced Structures (Clause 12)

F.1.2 Material Properties

Table 24 Material Properties

Youngs's Modulus Em	1500 MPa
Tangent Modulus	200MPa
Compression Strength fmc	2MPa
Tensile strength f_{mt}	0.1MPa
Volumetric mass	17kN/m3
Live load	2 KN/m2
Slabs and floor	Assumed C25/30 as per Eurocode 2 (EN 1992-1-1: Unreinforced Structures (Clause 12)

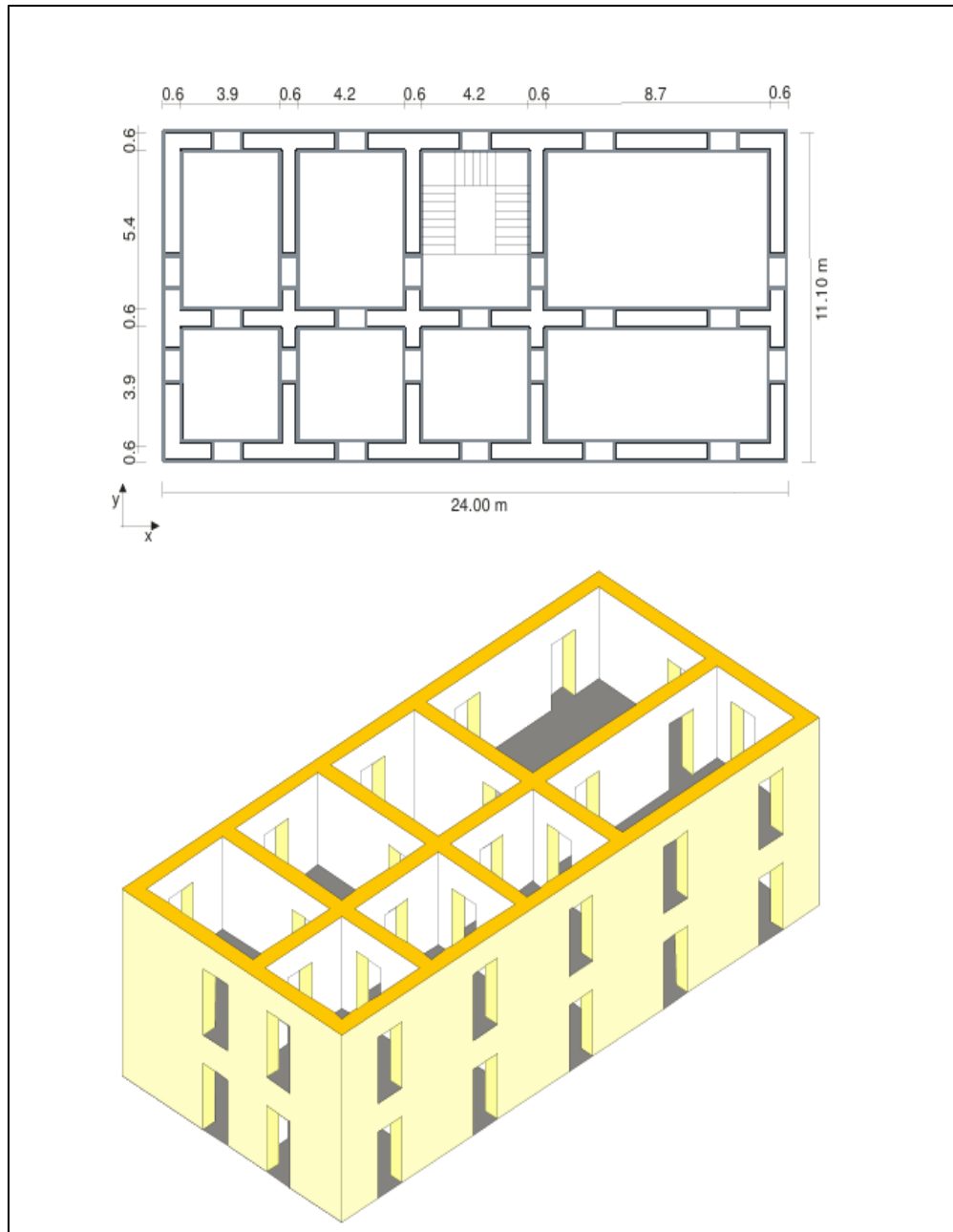## F.1.3 Plan given in Research paper and drafted in RFEM-6

Figure F.1.1 Layout of Plan given in research paper

F.1.4 Results of Validation

The finite element model of the building was replicated in RFEM-6 based on the structural plan from the research paper. A detailed comparison of mesh density, element types, and boundary conditions was carried out to ensure consistency between the referenced study and
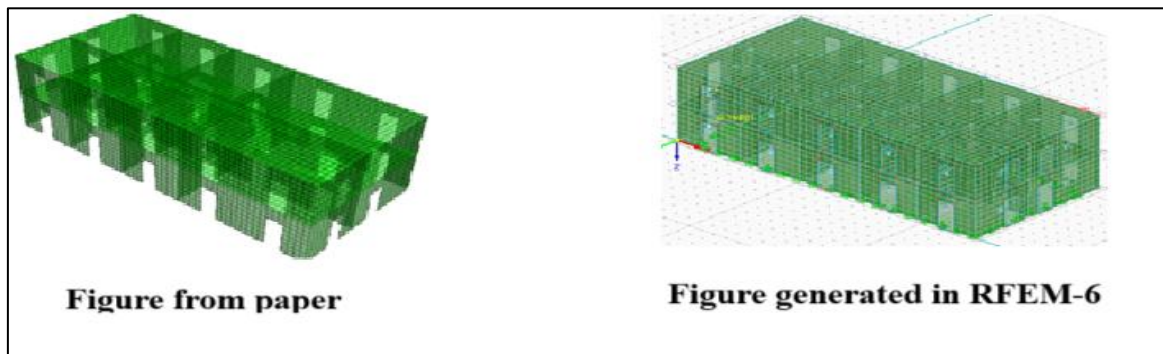
the developed model.

Figure F.1.2 Fem comparison of meshing

F.1.4.1 Results of mode shape of Research paper versus Result of RFEM
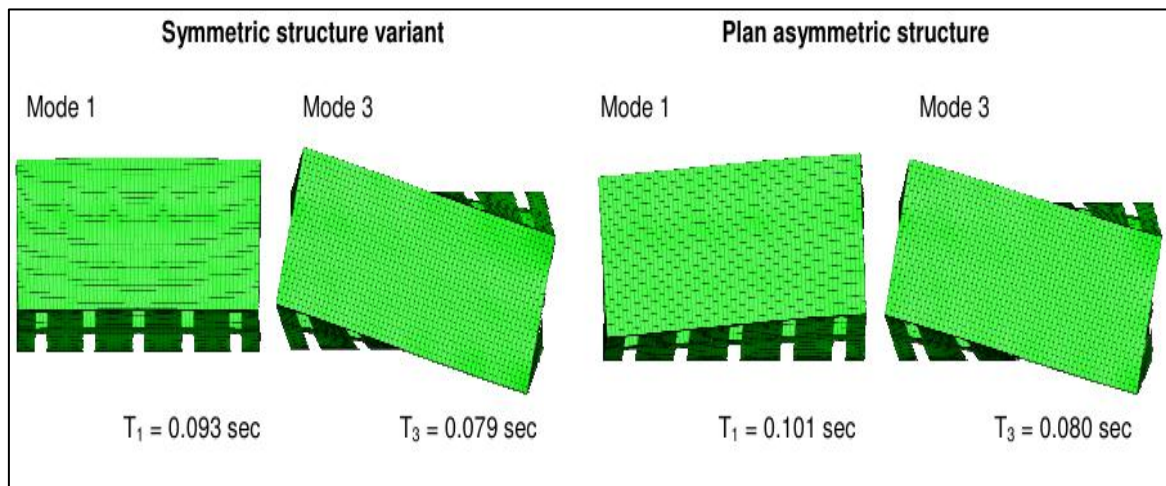

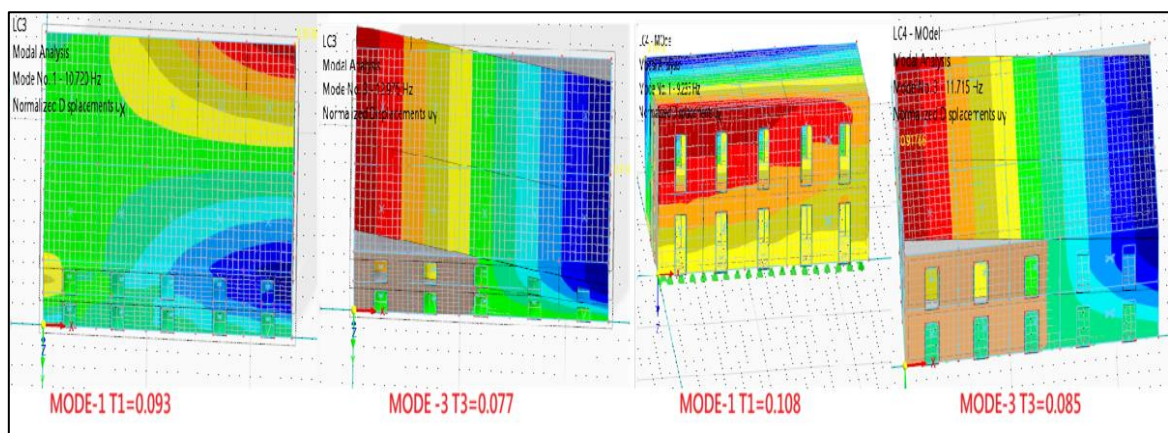Figure F.1. 3 Result of natural periods and Mode shape as per research paper

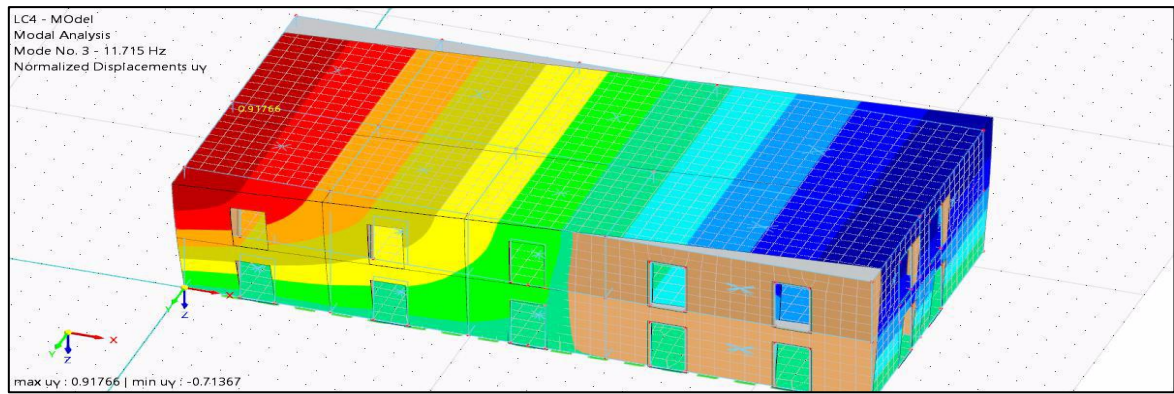Figure F.1.4 Result of natural periods and Mode shape as per RFEM 6

Figure F.1.5 Normalized displacement Uy of mode 3

F.1.4.2 Natural periods and mode of Vibrations of Building of Symmetrical building

Table 25 Modes and natural Time period for symmetrical plan

Mode No.	Eigen value λ [1/s2]	Angular Frequency ω [rad/s]	Natural Frequency f [Hz]	Natural Period T [s]	Result as Per Research paper
1	4536.779	67.356	10.720	0.093	Result of Mode 1=0.093
2	4940.813	70.291	11.187	0.089	
3	6646.364	81.525	12.975	0.077	Result of Mode 3 =0.079

Table 26 Result Error Percentage

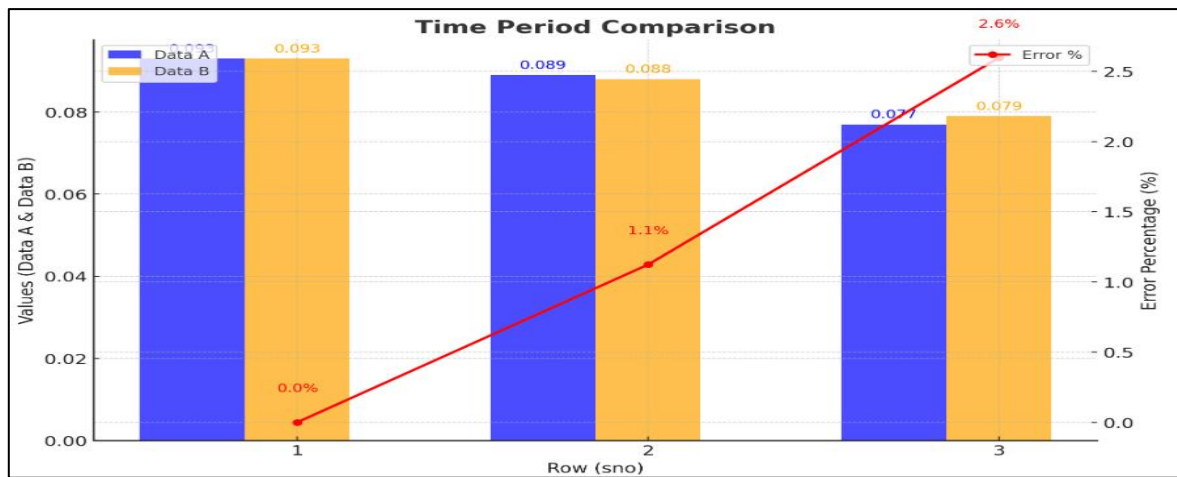| MODES	Research Paper	AS PER RFEM-6	ERROR %
1	0.093	0.093	0%
3	0.079	0.077	2.6%

Figure F.1.6 Represents error percentage for symmetrical plan

F.1.4.3 Natural periods and mode of Vibrations of Building of Asymmetrical Building

Table 27 Modes and natural Time period for Asymmetrical plan

Mode No.	Eigen value λ [1/s2]	Angular Frequency ω [rad/s]	Natural Frequency f [Hz]	Natural Period T [s]	RESULT AS PER RP
1	3366.591	58.022	9.235	0.108	Result of Mode 1=0.101
2	4340.592	65.883	10.486	0.095	
3	5417.774	73.606	11.715	0.085	Result of Mode 3 =0.080

Table 28 Result Error Percentage

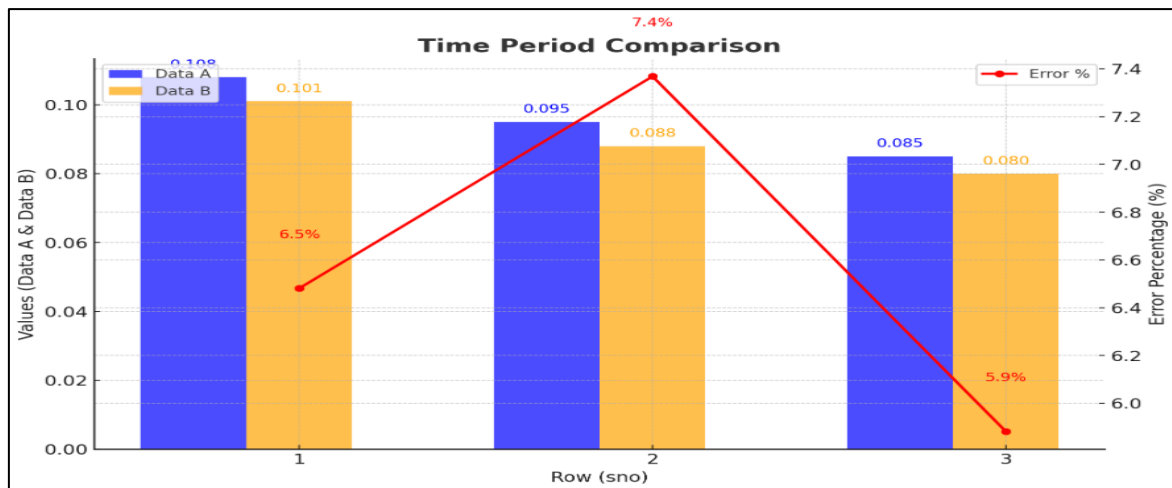| MODES	Research Paper	AS PER RFEM-6	ERROR %
1	0.101	0.108	6.5%
3	0.080	0.085	5.9%

Figure F.1.7 Represents error percentage for Asymmetrical plan

F.1.5 Base Shear Result:

Table 29 Base shear result

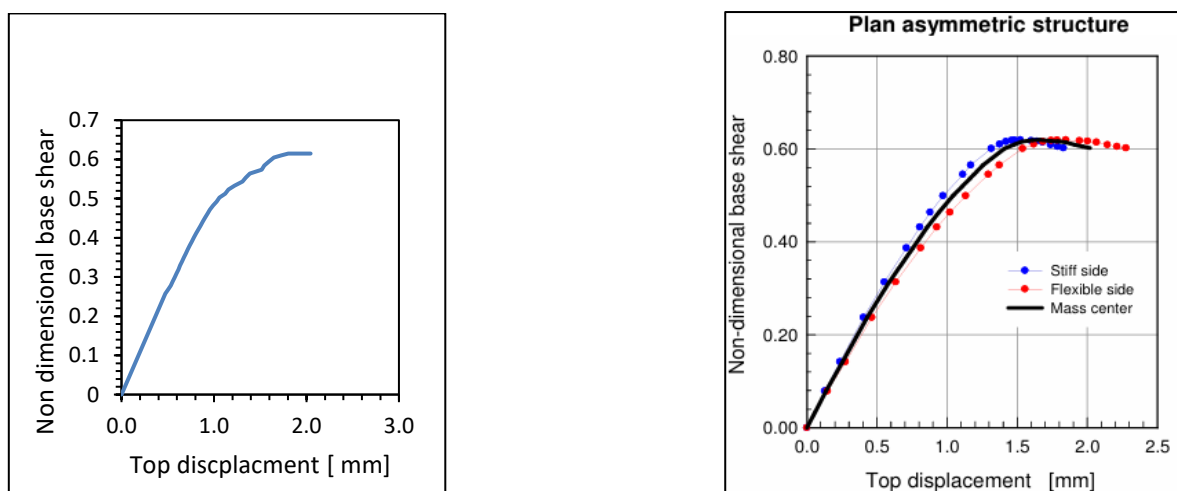| Non dimensional base shear (kN)	Research Paper	Present study	Error Percentage%
	0.630	0.645	2.33%

F.1.6 Pushover graph as per Paper versus Current study:

Figure F.1.8 Represents comparison of base shear